The thermodynamics of continuous feedback control

Case studies based on the quantum Fokker-Planck master equation

Joël Aschwanden
Master Thesis

Prof. Dr. Patrick Potts
Prof. Dr. Christoph Bruder
Kacper Prech

July 2023

We investigate the thermodynamics of three toy models to understand heat and work better. One is based on a classical particle following a random path given by an Ornstein-Uhlenbeck process, and two are based on using measurement backaction to put energy into a quantum system that can then be extracted by continuous feedback, creating a measurement-powered engine. The calculations of heat and work of the quantum systems are based on the quantum Fokker-Planck master equation introduced in [1], removing the necessity of using stochastic differential equations to describe systems under continuous feedback control.

1 Introduction

Quantum thermodynamics is an emerging research field aiming to extend standard thermodynamics and non-equilibrium statistical physics to ensembles of sizes well below the thermodynamic limit in non-equilibrium situations, and with the full inclusion of quantum effects [2]. In other words, it describes the relationship between two physical theories: thermodynamics and quantum physics.

One subfield of quantum thermodynamics describes open quantum systems with continuous feedback control. A detector measures a quantity of the system, and this measurement result is fed back to the system by changing experimental parameters such as applied electric fields. This process of the detector influencing the system and the system influencing the detector in return leads to a feedback loop between the quantum system and the detector, which both influence each other.

There has been progress in describing these systems in the past three decades [3]. However, these descriptions are typically based on stochastic differential equations, which often have to be solved numerically [4]. Because of this, they provide only limited qualitative insight; for example, their energetics are not yet fully understood [1].

To get more insight into systems with continuous feedback control, the letter "Quantum Fokker-Planck master equation for continuous feedback control" [1] presents a new formalism that allows the derivation of a master equation of the system alone. This change means that instead of a stochastic differential equation, which can mostly only be solved numerically, we have an ordinary differential equation that can be used to

get insight into the system's behavior.

A different subfield of quantum thermodynamics aims to optimize quantum machines that extract work from baths at different temperatures. One way of improving the extracted work is to include a Maxwell demon, an agent that uses information about the system to optimize work extraction [5]. Feedback control is an example of a Maxwell demon that can improve work extraction through the information gained by measuring the system [6]. So far, most of these quantum machines have used a heat bath as their primary source of energy. However, projective measurements on a quantum system can increase its average energy if the observable does not commute with the system's Hamiltonian [7]. This leads to a different approach being possible: using measurement as fuel in a new kind of quantum engine.

One example of such a measurement-powered engine was discussed in [8]. This paper discussed a system with no thermal bath where energy was put into the system using measurement backaction, and then a drive Hamiltonian was used to extract work. The setup discussed was to prepare a quantum system in a starting state with high energy and then use the drive to extract work for some time. Afterward, a projective measurement and, if necessary, a feedback pulse prepares the state back to its starting state.

We aim to extend the idea of putting energy into a system via measurement backaction, which can then be extracted as work to quantum systems under continuous feedback control. Instead of measurement and work extraction done separately, they are done simultaneously. We discuss two quantum toy models that could be used as measurement-powered engines. In a quantum system under continuous feedback control, the measurement backaction, which can change the average energy of the system, leads to an additional term in the average energy change of the system that does not behave like heat or work. We call this new component "change in measurement energy." Sometimes, this term is also called *quantum heat* [9].

In the project thesis "The Thermodynamics of continuous feedback control" [10], we introduced suitable definitions of heat, work, and change in measurement energy for quantum systems under feedback control and systems described by quantum master equations. In Sec. 2, we introduce the necessary theoretical knowledge to calculate the thermodynamics of these systems.

In this thesis, we discuss three toy models to get further insight into the thermodynamics of measurement and feedback systems where we use the results of [1] and [10] to calculate heat, work, and change in measurement energy in these toy models and find ways to maximize the extracted work.

The first system we discuss is a model of a classical particle in Sec. 3 that follows a random path given by an Ornstein-Uhlenbeck process. This process is an example that demonstrates how introducing randomness into a system changes power and work in the system. We do compare two protocols here: a deterministic and a stochastic one. The main result of this model is the calculation of heat and work and the discussion of the newly introduced drift and diffusion terms that arise due to the stochastic nature of the process in Sec. 3.3.2.

The second discussed system found in Sec. 4.1 is based on the measurement-powered engine discussed above [8]. The system we discuss in Sec. 4.1 is a continuous version of said protocol. We use a measurement-dependent drive to extract work while the measurement backaction continuously puts energy into the system through a change in measurement energy. The main results of this system are the calculated steady state and extracted work and change in measurement energy in the steady state discussed in Sec. 4.1.4. We also provide an analytic calculation of the system state in the fast detector limit in Sec. 4.1.5.

The third system found in Sec. 4.2 expands on the idea of the second system by removing the time dependence of the Hamiltonian. Instead of using a measurement-dependent drive to extract work, we use measurement feedback to keep the ground state of the system close to the position of the current system state. This means when the measurement backaction increases the system's energy, the Hamiltonian changes the ground state to again be close to the system state. This decreases the system's energy and lets us extract work from the system. Here, the main results are the calculated steady state and the extracted work and change in measurement energy found in Fig. 17. We also did an analytic calculation of the system state in the fast detector limit in Sec. 4.3.

2 Heat and Work in Quantum systems

We introduce the analytical background on calculating heat and work in systems described by a quantum master equation and later in feedback systems described by a Quantum Fokker-Planck master equation [1].

We will then use the results of this chapter to calculate heat and work in multiple toy models found in Sec. 3 and Sec. 4. Further details can be found in [10].

2.1 Heat and work in Quantum master equations

We consider a quantum system described by a density matrix $\hat{\rho}$ connected to several baths. We describe the time-evolution of the system by a quantum master equation

$$\partial_t \hat{\rho}(t) = -i[\hat{H}(D(t)), \hat{\rho}(t)] + \mathcal{L}_B \hat{\rho}(t) \equiv \mathcal{L}(D(t))\hat{\rho}(t). \tag{1}$$

Here, the first term describes the system's unitary time evolution, and the second term describes the time evolution produced by the system's energy exchange with the baths [11].

2.1.1 Deterministic protocol

Here, the Hamiltonian is dependent on some deterministic function $D(t)$, which will later represent the measurement outcome of a system under continuous feedback control.

In this system, the average energy change can be split up into heat and work [2]

$$\partial_t \operatorname{Tr}\{\hat{H}(D(t))\hat{\rho}(t)\} \equiv \partial_t \left\langle \hat{H}(D(t)) \right\rangle = \partial_t D(t)\langle \partial_D \hat{H}(D(t))\rangle + \operatorname{Tr}\{\hat{H}(D(t))\partial_t\hat{\rho}(t)\} = \langle P \rangle + \langle J \rangle. \tag{2}$$

where heat current and power are defined as

$$\langle P \rangle \equiv \partial_t D(t) \left\langle \partial_D \hat{H}(D(t)) \right\rangle, \qquad \langle J \rangle \equiv \operatorname{Tr}\{\hat{H}(D(t))\partial_t\hat{\rho}\} = \operatorname{Tr}\{\hat{H}(D(t))\mathcal{L}_B\hat{\rho}(t)\}. \tag{3}$$

The formal definitions of the average heat absorbed by the system after time τ and average work done on the system after time τ are then

$$\langle Q \rangle \equiv \int_0^\tau \operatorname{Tr}\{\hat{H}(D(t))\mathcal{L}_B\hat{\rho}(t)\}dt, \qquad \langle W \rangle \equiv \int_0^\tau \partial_t D(t)\langle \partial_D \hat{H}(D(t))\rangle dt. \tag{4}$$

In the steady state, we have $\partial_t\langle \hat{H}(D(t))\rangle = 0$. This means either power is dissipated or heat is turned into work. In more detail, $\langle J \rangle$ has to be negative in the steady state. A positive average heat current would lead to a positive entropy production rate, which is impossible in the steady state because of the second law of thermodynamics [2].

The average energy change comprises two types of energy transfer. Their intuitive meaning is that of two types of energetic resources, one fully controllable and useful, the other uncontrolled and wasteful [2]. Generally, an experimenter controls the variation of $\hat{H}$, which is why the energy change associated with the variation of $\hat{H}$ is associated with work. The uncontrollable energy change is associated with reconfiguring the system state $\hat{\rho}_t$ and is associated with heat.

2.1.2 Stochastic protocol

Next, we consider the function D to be random and follow a stochastic differential equation

$$dD = A(D)dt + B(D)dW. \tag{5}$$

Solutions to stochastic differential equations are not functions but trajectories $D(t)$ that depend on the specific realization of the noise dW [12]. dW is called the *Wiener increment* which is an infinitesimal Gaussian increment with variance dt and mean zero. This means if we want to obtain one of the possible paths for D in each timestep dt, we produce a random value for dW and then calculate $D(t + dt)$ with

$$D(t + dt) = D(t) + dD = D(t) + A(D(t))dt + B(D(t))dW. \tag{6}$$

This added randomness by introducing the Wiener increment dW leads to quite a few changes in how things are calculated in stochastic calculus. For example, when doing a Taylor series expansion of $\hat{H}(D)$, we must consider second-order terms in the limit $dt \to 0$

$$d\hat{H}(D) = \partial_D \hat{H}(D)dD + \frac{1}{2}\partial_D^2 \hat{H}(D)dD^2, \qquad dD^2 = B(D)^2 dt. \tag{7}$$

These second-order terms do not vanish based on the variance of dW. The variance being dt also leads to Ito's rule [12]

$$(dW)^2 = dt. \tag{8}$$

Ito's rule is also the reason why $dD^2 \neq 0$ but instead $dD^2 = B(D)^2 dt$. It also means we have to include a third term in the average energy change because, in the product rule, there is now a third term appearing.

$$\partial_t \left\langle \hat{H}(D) \right\rangle = \frac{E(\text{Tr}\{d(\hat{H}(D)\hat{\rho}_c)\})}{dt} = \frac{1}{dt}\left(E(\text{Tr}\{d\hat{H}(D)\hat{\rho}_c + \hat{H}(D)d\hat{\rho}_c + d\hat{H}(D)d\hat{\rho}_c\}) \right). \tag{9}$$

In this stochastic setting, our average differs from the standard quantum mechanical average in Sec. 2.1.1. Here, $E(\cdot)$ denotes the average over all outcome of D.

From the differential equation for $\hat{\rho}_t$ mentioned in Eq. (1) we get

$$d\hat{\rho}_c = -i[\hat{H}(D(t)), \hat{\rho}_c]dt + \mathcal{L}_B\hat{\rho}_c dt. \tag{10}$$

Here, $\hat{\rho}_c$ is the conditional density matrix, which depends on the history of values of D.

The third term $\frac{1}{dt}E(\text{Tr}\{d\hat{H}(D(t))d\hat{\rho}_c\})$ vanishes because $d\hat{\rho}_c$ has no direct dependence on dW, as seen in Eq. (10). This term will become important in Sec. 2.2 when introducing measurement feedback where $\hat{\rho}_c$ directly depends on dW.

This means we are left with two contributions to the average energy change. Again, we say that the energy change associated with a change in the Hamiltonian $\hat{H}(D)$ is work, and the energy change associated with a change in the system state $\hat{\rho}_c$ is heat;

$$\langle P \rangle = \frac{1}{dt}E(\text{Tr}\{d\hat{H}(D)\hat{\rho}_c\}) = \left\langle A(D)\partial_D \hat{H}(D) \right\rangle + \frac{1}{2}\left\langle B^2(D)\partial_D^2 \hat{H}(D) \right\rangle,$$
$$\langle J \rangle = \frac{1}{dt}E(\text{Tr}\{\hat{H}(D)d\hat{\rho}_c\}) = E(\text{Tr}\{\hat{H}(D)\mathcal{L}_B\hat{\rho}_c\}). \tag{11}$$

To summarize, the additional randomness of D introduces a second term for the work. We will call the first term the *drift term* because it depends on the change of the Hamiltonian. The second term we call *diffusion term* because it is the term that is introduced by the newly added randomness of the process.

We again have $\partial_t\langle \hat{H}(D)\rangle = 0$ in the steady state. This means either power is dissipated or heat is turned into work. What is new is that we can have energy exchanges without a bath. Because the work now consists of the drift and diffusion terms, we can have energy exchanges between both of these terms in the steady state. An example of this can be found in Sec. 3.3.

2.2 Heat and Work in Quantum Fokker-Planck master equations

Now, we focus on heat and work in a quantum system under feedback control [1]. The system we look at is an open quantum system whose dynamics are described by a Liouville superoperator $\mathcal{L}(D)$ given in Eq. (1). Instead of having a general function $D(t)$, we continuously measure a system observable $\hat{A}$ and use the measurement result as the function $D(t)$. Feedback control is achieved by continuously feeding back the measurement results into the system via the Liouville superoperator $\mathcal{L}(D)$.
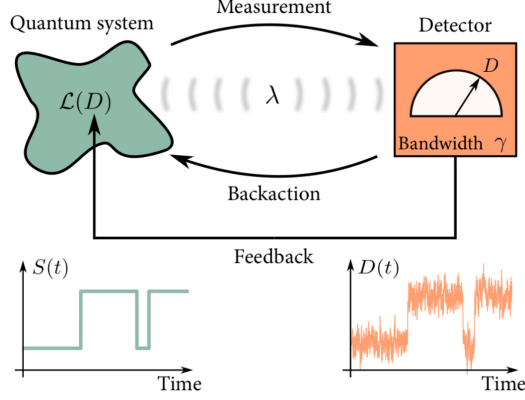
Figure 1: Overview of the measurement and feedback setup. It consists of an open quantum system and a detector with finite bandwidth γ continuously measuring a system observable. The measurement strength λ determines the magnitude of the measurement backaction. The measurement result D is brought back into the system via the Liouville superoperator $\mathcal{L}(D)$. The time traces visualize the evolution of the state $S(t)$ and measurement outcome $D(t)$ over time. The figure is taken from [1].

The measurement is not necessarily projective; instead, the parameter λ determines the measurement strength. The limit $\lambda \to \infty$ corresponds to a strong projective measurement, while the limit $\lambda \to 0$ corresponds to a weak, non-intrusive measurement. A weak measurement reduces measurement backaction and preserves quantum coherence but increases measurement uncertainty [1].

A realistic detector description is achieved by introducing finite bandwidth γ, which acts as a low-pass frequency filter [13]. This filters out high-frequency measurement noise of the measurement outcome but introduces a time delay that scales with $1/\gamma$. This time delay is illustrated in Fig. 1. While the system state $S(t)$ jumps between states, the filtered measurement outcome D needs some time to reach the new measurement outcome and is then stable again within the measurement uncertainty.

To describe this system, we introduce a density operator $\hat{\rho}_t(D)$ describing the joint state of the system and detector. This density operator is a joint probability density for both the system state $\hat{\rho}_t$ and detector state D.

Averaging out the possible measurement outcomes $\int \hat{\rho}_t(D)\, dD = \hat{\rho}_t$ gives us the system state for an unknown measurement outcome. We can also extract the probability distribution $P(D,t)$ of the measurement outcomes by taking the trace $\mathrm{Tr}\{\hat{\rho}_t(D)\} = P(D,t)$. If we want to know the system state after measuring a certain measurement outcome, we have to renormalize the density operator: $\hat{\rho}_t(D)/P(D,t)$.

The evolution of $\hat{\rho}_t(D)$ is given by the following Fokker-Planck master equation [1].

$$\partial_t \hat{\rho}_t(D) = \mathcal{L}(D)\hat{\rho}_t(D) + \lambda \mathcal{D}[\hat{A}]\hat{\rho}_t(D) - \gamma \partial_D \mathcal{A}(D)\hat{\rho}_t(D) + \frac{\gamma^2}{8\lambda}\partial_D^2 \hat{\rho}_t(D),$$

$$\mathcal{D}[\hat{A}]\hat{\rho} = \hat{A}\hat{\rho}\hat{A}^\dagger - \frac{1}{2}\{\hat{A}^\dagger \hat{A}, \hat{\rho}\}, \quad \mathcal{A}(D)\hat{\rho} = \frac{1}{2}\{\hat{A} - D, \hat{\rho}\}. \tag{12}$$

The first term describes the system's evolution, the second describes how the system dephases into the eigenbasis of $\hat{A}$ proportional to λ due to measurement backaction, and the last two terms consist of a Fokker-Planck equation describing the evolution of the detector. This Fokker-Planck equation describes an Ornstein-Uhlenbeck process with system-dependent drift coefficient $\gamma \mathcal{A}(D)$ and diffusion constant $\gamma^2/8\lambda$ [14]. This Ornstein-Uhlenbeck process describes the drift of the filtered measurement outcome towards a value determined by the system state. The drift speed is proportional to γ, which explains the introduced time delay that scales with $1/\gamma$. We also see why a weak measurement introduces measurement uncertainty as the diffusion term scales with $1/\lambda$. Further details on an Ornstein-Uhlenbeck process can be found in Sec. 3.3.2.

We are interested in the thermodynamics of measurement and feedback systems, so we would like to be able to calculate heat and work in these systems. To achieve this, we calculate the average energy change $\partial_t \langle \hat{H}(D) \rangle \equiv \partial_t \operatorname{Tr} \left\{ \int dD \hat{H}(D) \hat{\rho}_t(D) \right\}$ based on the Fokker-Planck master equation [10]

$$\partial_t \left\langle \hat{H}(D) \right\rangle = \operatorname{Tr} \left\{ \int dD \hat{H}(D) \mathcal{L}_B \hat{\rho}_t(D) \right\} + \left\langle \lambda \mathcal{D}[\hat{A}] \hat{H}(D) + \gamma \mathcal{A}(D) \partial_D \hat{H}(D) + \frac{\gamma^2}{8\lambda} \partial_D^2 \hat{H}(D) \right\rangle. \tag{13}$$

If we now compare the terms with Eq. (11), the average energy change in the stochastic protocol, we see that three of the four terms here are familiar. The first term in Eq. (13) is similar to the heat in the stochastic protocol, and the two last terms are similar to the work of said protocol. The second term is new and results from the newly introduced measurement backaction and randomness of the measurement result. Going forward, we call this term a change in *measurement energy*. This component is sometimes also called *quantum heat* [9].

We now define heat and work in a way that makes the definitions similar to Eq. (11)

$$\langle P \rangle = \gamma \left\langle \mathcal{A}(D) \partial_D \hat{H}(D) \right\rangle + \frac{\gamma^2}{8\lambda} \left\langle \partial_D^2 \hat{H}(D) \right\rangle,$$

$$\langle J \rangle = \operatorname{Tr} \left\{ \int \hat{H}(D) \mathcal{L}_B \hat{\rho}_t(D) \, dD \right\},$$

$$\langle \dot{E}_{\mathrm{M}} \rangle = \lambda \left\langle \mathcal{D}[\hat{A}] \hat{H}(D) \right\rangle. \tag{14}$$

We want to understand better where these terms come from, so we take a step back and use stochastic calculus. The Fokker-Planck master equation Eq. (12) is based on the Belavkin equation, which is a stochastic differential equation for the conditional density matrix $\hat{\rho}_c$ [15]

$$d\hat{\rho}_c = \mathcal{L}(D) \hat{\rho}_c dt + \lambda \mathcal{D}[A] \hat{\rho}_c dt + \sqrt{\lambda} \{ \hat{A} - \langle \hat{A} \rangle_c, \hat{\rho}_c \} dW, \qquad \langle \hat{A} \rangle_c = \operatorname{Tr} \{ \hat{A} \hat{\rho}_c(t) \}. \tag{15}$$

Based on the Belavkin equation, we can calculate the average energy change using stochastic calculus

$$\partial_t \left\langle \hat{H}(D) \right\rangle = \frac{E(\operatorname{Tr} \{ d(\hat{H}(D) \hat{\rho}_c) \})}{dt} = \frac{1}{dt} \left(E(\operatorname{Tr} \{ d\hat{H}(D) \hat{\rho}_c + \hat{H}(D) d\hat{\rho}_c + d\hat{H}(D) d\hat{\rho}_c \}) \right). \tag{16}$$

In Seq. 2.1.2, the contribution of $\frac{1}{dt} E(\operatorname{Tr} \{ d\hat{H}(D(t)) d\hat{\rho}_c \})$ did vanish because $\hat{\rho}_c$ did not have a direct dependence on the Wiener increment dW. Here, we need to consider the contribution of this term.

We find the following contributions toward the average energy change [10]

$$\frac{1}{dt} (E(\operatorname{Tr} \{ d\hat{H}(D) \hat{\rho}_c \})) = \gamma \langle \hat{A} \rangle_c \left\langle \partial_D \hat{H}(D) \right\rangle - \gamma \left\langle D \partial_D \hat{H}(D) \right\rangle + \frac{\gamma^2}{8\lambda} \left\langle \partial_D^2 \hat{H}(D) \right\rangle,$$

$$\frac{1}{dt} (E(\operatorname{Tr} \{ \hat{H}(D) d\hat{\rho}_c \})) = E(\operatorname{Tr} \{ \hat{H}(D) \mathcal{L}_B \hat{\rho}_c \}) + \lambda \left\langle \mathcal{D}[\hat{A}] \hat{H}(D) \right\rangle,$$

$$\frac{1}{dt} (E(\operatorname{Tr} \{ d\hat{H}(D) d\hat{\rho}_c \})) = \frac{\gamma}{2} \left\langle \partial_D \hat{H}(D) \hat{A} \right\rangle + \frac{\gamma}{2} \left\langle \hat{A} \partial_D \hat{H}(D) \right\rangle - \gamma \langle \hat{A} \rangle_c \left\langle \partial_D \hat{H}(D) \right\rangle. \tag{17}$$

We can see that the middle line $\frac{1}{dt} (E(\operatorname{Tr} \{ \hat{H}(D) d\hat{\rho}_c \}))$, which represents the influence of the change of the system state, is responsible for both heat and change in measurement energy. We also see that we need to combine the first and third lines to get our definition of the work in Eq. (14). This is surprising as in Seq. 2.1.2, we did say that the average energy change associated with a change in the Hamiltonian $\hat{H}(D)$ is work, and here, work is also dependent on a term that is also associated with a change in the system state.

There is an intuitive explanation for why this term is part of the work. In a system under measurement and feedback control in a single timestep dt, the measurement of the system happens first, changing the system state via measurement backaction and evolution of the Hamiltonian. Then, after the measurement, the measurement result is fed back into the system, changing the Hamiltonian of the system. Since the system state is already changed at that point, the change of the Hamiltonian produces an additional term

$d\hat{H}d\hat{\rho}_c$. This idea can be illustrated as

$$
\begin{array}{cccc}
t & & \longrightarrow & t + dt \\
\hat{H} \longrightarrow & & \hat{H} \longrightarrow & \hat{H} + d\hat{H} \\
\hat{\rho}_c \longrightarrow & & \hat{\rho}_c + d\hat{\rho}_c \longrightarrow & \hat{\rho}_c + d\hat{\rho}_c \\
\mathrm{Tr}\{\hat{H}\hat{\rho}_c\} \longrightarrow & \mathrm{Tr}\{\hat{H}(\hat{\rho}_c + d\hat{\rho}_c)\} \longrightarrow & \mathrm{Tr}\{(\hat{H} + d\hat{H})(\hat{\rho}_c + d\hat{\rho}_c)\},
\end{array}
\tag{18}
$$

$$
\Rightarrow d\,\mathrm{Tr}\{\hat{H}\hat{\rho}_c\} = \mathrm{Tr}\{\hat{H}d\hat{\rho}_c\} + \mathrm{Tr}\{d\hat{H}\hat{\rho}_c + d\hat{H}d\hat{\rho}_c\}.
$$

In this calculation, we can see that the first step of changing only the system state is responsible for the term $\hat{H}d\hat{\rho}_c$, which in the end turns into the terms of heat and change in measurement energy. The second step of changing the Hamiltonian produces an additional term $d\hat{H}d\hat{\rho}_c$. It makes sense to include this term in the definition of the work because it is a result of the part of the timestep where we change the Hamiltonian, which we said is associated with work.

2.2.1 Time-dependent Hamiltonian

In Seq. 4.1, we will work with a toy model that has a time-dependent Hamiltonian $\hat{H}(D,t)$ because of the product rule; this adds another term to the average energy change

$$
\partial_t \left\langle \hat{H}(D,t) \right\rangle = \left\langle \partial_t \hat{H}(D,t) \right\rangle + \mathrm{Tr}\left\{ \int dD \hat{H}(D,t)\partial_t \hat{\rho}_t(D) \right\}.
\tag{19}
$$

It makes sense to associate it with work since it shows up because of a new change in the Hamiltonian. This means the power for a time-dependent Hamiltonian reads

$$
\langle P \rangle = \gamma \left\langle \mathcal{A}(D)\partial_D \hat{H}(D) \right\rangle + \frac{\gamma^2}{8\lambda} \left\langle \partial_D^2 \hat{H}(D) \right\rangle + \left\langle \partial_t \hat{H}(D,t) \right\rangle.
\tag{20}
$$

2.2.2 Fast detector limit for linear feedback

In the case of the detector timescale $1/\gamma$ being much shorter than the system timescale $1/T$; $\gamma \gg T$, one can derive a Markovian master equation for the system state to first order in $1/\gamma$ [1].
Here, we will introduce this master equation in the case where $\gamma \to \infty$ and in the case of linear feedback. For this, we consider a feedback Liouvillian of the form

$$
\mathcal{L}_\lambda(D)\hat{\rho} = \mathcal{L}\hat{\rho} + \lambda\mathcal{D}[\hat{A}] - iD[\hat{F}, \hat{\rho}].
\tag{21}
$$

This form corresponds to a system under linear feedback control as the operator $\hat{F}$ is not D dependent. In the limit $\gamma \to \infty$, Eq. (12) simplifies to a Markovian master equation for the system state $\hat{\rho}_t$ [16]

$$
\partial_t \hat{\rho}_t = \left[\mathcal{L}_0 + \lambda\mathcal{D}[\hat{A}] + \gamma^{-1}\mathcal{L}_{\mathrm{corr}} \right] \hat{\rho}_t.
\tag{22}
$$

where for the zeroth order, we have

$$
\mathcal{L}_0\hat{\rho} = \mathcal{L}\hat{\rho} - i[\hat{F}, \mathcal{A}\hat{\rho}], \qquad \mathcal{A}\hat{\rho} = \frac{1}{2}\{\hat{A}, \hat{\rho}\}.
\tag{23}
$$

The correction simplifies to

$$
\gamma^{-1}\mathcal{L}_{\mathrm{corr}} = \frac{1}{4\lambda}\mathcal{D}[\hat{F}]\hat{\rho}.
\tag{24}
$$

In Eq. (22), the first term describes the system's evolution, and the second describes how the system dephases into the eigenbasis of $\hat{A}$ due to measurement backaction. The new third term also describes a dephasing but in the eigenbasis of $\hat{F}$ proportional to $1/4\lambda$.
We see that a term of $\mathcal{L}_{\mathrm{corr}}$ is linear in γ contributing to the infinite bandwidth limit. The reason for this is that with infinite bandwidth, the measurement outcomes D may become infinitely large which leads to a term in the feedback Liouvillian, Eq. (21), that becomes infinitely large.
An infinite bandwidth also means that the drift of the filtered measurement outcome toward a value determined by the system becomes infinitely fast. We will call the limit $\gamma \to \infty$ the "fast detector limit."

3 Classical particle

The systems encountered in feedback control we want to understand further evolve randomly over time. First, we look at a simpler system of a classical particle whose position evolves first deterministically and, in a second step, randomly over time.

We look at a classical particle whose energy depends on its position D.

$$E(D) \equiv H(D). \tag{25}$$

3.1 Deterministic case

In this section, we consider a deterministic path for our particle. The particle follows some path $D(t)$ starting at $D(0) = D_i$ and ending at $D(\tau) = D_f$. We will consider the work in the interval $[0, \tau]$

$$
\begin{aligned}
W = \int_0^\tau P \, dt &= \int_0^\tau \partial_t D(t) \partial_D H(D(t)) \, dt \\
&= \int_0^\tau \frac{d}{dt} H(D(t)) \, dt \\
&= H(D(\tau)) - H(D(0)).
\end{aligned}
\tag{26}
$$

Here, we used Eq. (3) to calculate the work. There is no heat here as the system is not connected to a bath.

3.2 Stochastic case

Instead of a deterministic path, the particle follows a random path $D(t)$ with a starting point $D(0) = D_i$. This makes the system more complicated as instead of some predetermined path, the system follows random paths determined by Eq. (5).

For a stochastic differential equation of this form, we can calculate the average power produced at a certain time with Eq. (11)

$$\langle P \rangle = \langle A(D,t) \partial_D H(D) \rangle + \frac{1}{2} \langle B^2(D,t) \partial_D^2 H(D) \rangle. \tag{27}$$

As introduced in Sec. 2.1, we call the first term *drift term* and the second *diffusion term*. We can calculate the average work in the interval $[0, \tau]$ with

$$\langle W \rangle = \int_0^\tau \langle P \rangle dt = \int_0^\tau dt \langle A(D,t) \partial_D H(D) \rangle + \frac{1}{2} \langle B^2(D,t) \partial_D^2 H(D) \rangle. \tag{28}$$

If we now know the probability distribution $F(D,t)$ for D, we can rewrite the expectation values to

$$\langle W \rangle = \int_0^\tau \langle P \rangle dt = \int_0^\tau dt \int_{-\infty}^{\infty} dD A(D,t) \partial_D H(D) F(D,t) + \frac{1}{2} B^2(D,t) \partial_D^2 H(D) F(D,t). \tag{29}$$

Now we integrate by parts and use that $\lim_{D \to \infty} F(D,t) = 0$ and $\lim_{D \to \infty} \partial_D F(D,t) = 0$.

$$\langle W \rangle = \int_0^\tau dt \int_{-\infty}^{\infty} dD H(D) \left(-\partial_D (A(D,t) F(D)) + \frac{1}{2} \partial_D^2 (B^2(D,t) F(D,t)) \right). \tag{30}$$

For a stochastic differential equation in the form of Eq. (5), one can derive a Fokker-Planck equation for its probability distribution $F(D)$. The proof of this can be found in App. A.

$$\partial_t F(D,t) = -\partial_D (A(D,t) F(D,t)) + \frac{1}{2} \partial_D^2 (B^2(D,t) F(D,t)). \tag{31}$$

Therefore, we can rewrite the work into

$$\langle W \rangle = \int_{-\infty}^{\infty} dD \, H(D) \int_0^\tau dt \, \partial_t F(D,t) \tag{32}$$

$$= \int_{-\infty}^{\infty} dD \, H(D)(F(D,\tau) - F(D,0)) \tag{33}$$

$$= \langle H(D(\tau)) \rangle - \langle H(D(0)) \rangle. \tag{34}$$

Since we have no heat here, the average energy change over the interval $[0, \tau]$ is also the average work.

3.3 Informative example

In this section, we go through an example of a classical particle whose energy depends on its position D.
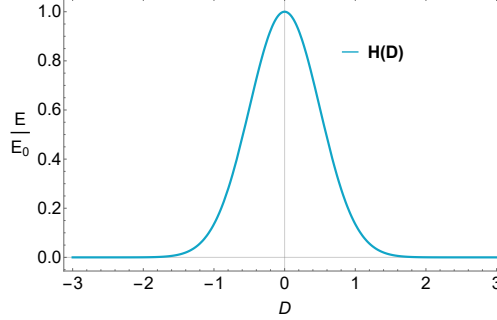
$$E(D) = E_0 e^{-\alpha D^2} \equiv H(D). \tag{35}$$

Figure 2: Energy $E(D)$ of the particle dependent on its position D. This plot was made with $\alpha = 2$. Higher/lower values of α correspond to a narrower/wider function.

3.3.1 Deterministic case

The particle follows some path $D(t)$ starting at $D(0) = D_i$ and ending at $D(\tau) = D_f$. We consider the work in the interval $[0, \tau]$

$$W = \int_0^\tau P \, dt = \int_0^\tau \partial_t D(t) \partial_t H(D(t)) \, dt \tag{36}$$

$$= \int_0^\tau \partial_t D(t) \left(-E_0 2\alpha e^{-\alpha D^2} \right) dt \tag{37}$$

$$= E_0 e^{-\alpha D^2} \Big|_0^\tau = E_0 \left(e^{-\alpha D_f^2} - e^{-\alpha D_i^2} \right) \tag{38}$$

$$= H(D(\tau)) - H(D(0)). \tag{39}$$

Which is what we expected based on Sec. 3.1. The work done in the interval $[0, \tau]$ is the difference in the Hamiltonian at the start and end of the time interval.

3.3.2 Stochastic case

We now consider a random path $D(t)$ for the particle with starting point $D(0) = D_i$ drifting towards D_f with a rate γ. This behavior is described with an Ornstein-Uhlenbeck process

$$dD = \gamma(D_f - D)dt + \sigma dW. \tag{40}$$

Here, σ tells us how large the influence of the Wiener increment dW is. This process is an example of a stochastic differential equation that is solvable analytically. At each time t, the particle's position is normally distributed around its expected position. The proof of this can be found in App. B.

$$D(t) \sim \mathcal{N} \left(D_i e^{-\gamma t} + D_f (1 - e^{-\gamma t}), \frac{\sigma^2}{2\gamma}(1 - e^{-2\gamma t}) \right). \tag{41}$$

Here the notation $D(t) \sim \mathcal{N}(\mu, \Sigma^2)$ stands for $D(t)$ being normally distributed around the mean $\mu = \langle D(t) \rangle$ with variance $\Sigma^2 = V(D(t))$.

Based on Eq. (27), we can calculate the average power for each time with the following expression.

$$\langle P \rangle = \langle \gamma(D_f - D)\partial_D H(D)\rangle + \frac{1}{2}\langle \sigma^2 \partial_D^2 H(D)\rangle$$

$$= \langle \gamma(D_f - D)(-2\alpha E_0 D e^{-\alpha D^2})\rangle + \frac{1}{2}\langle \sigma^2 2\alpha E_0(e^{-\alpha D^2} - 2\alpha D^2 e^{-\alpha D^2})\rangle. \tag{42}$$

Since we know the distribution of D for each time, these expectation values can be written as

$$\langle f(D(t))\rangle = \int_{-\infty}^{\infty} f(D)\frac{1}{\sqrt{V(D(t))}\sqrt{2\pi}}e^{-\frac{1}{2}\left(\frac{D-\langle D(t)\rangle}{\sqrt{V(D(t))}}\right)^2} dD, \ \forall t \in [0, \tau]. \tag{43}$$

In the following, we will compare the power in Eq. (42) to the *deterministic power*, which corresponds to the power of the same process but without any randomness. This is achieved by setting $\sigma = 0$ in the stochastic differential equation for D. This leads to a deterministic path.

$$D_{det}(t) = D_i e^{-\gamma t} + D_f(1 - e^{-\gamma t}). \tag{44}$$

The power then becomes the following.

$$P_{det} = \gamma(D_f - D_{det}(t))(-2\alpha E_0 D_{det}(t)e^{-\alpha D^2}). \tag{45}$$

Now we calculate the average power for all time for the Ornstein Uhlenbeck process that starts in $D_i = -1$ and drifts towards $D_f = 1$. The result of this is shown in Fig. 3.
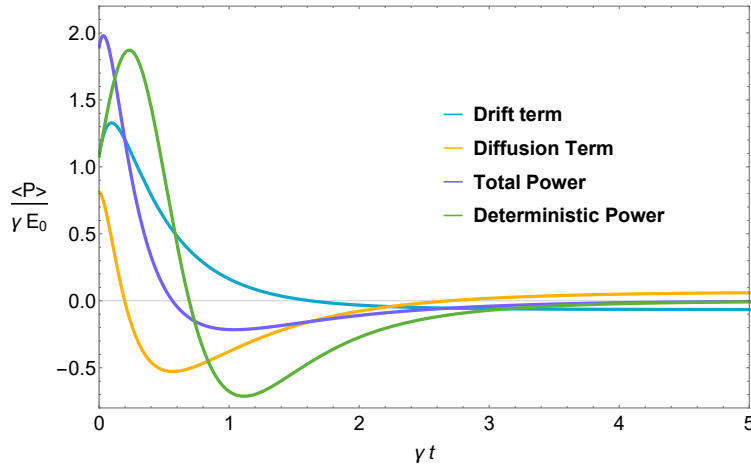

Figure 3: Average power as a function of time t. Here, we compare the average total power with the deterministic power produced in the same process with $\sigma = 0$. Drift and diffusion terms refer to the first and second terms in Eq. (42). The choice for the parameters here is $\gamma = 1$, $\sigma = 1$, $\alpha = 2$, $E_0 = 1$, $D_i = -1$ and $D_f = 1$.

The behavior of the power over time can be explained when looking at both Fig. 3 and Fig. 4. We see that the drift term starts positive and, over time, becomes negative. This makes sense when looking at Fig. 4. The function inside the expectation value over D exhibits a similar sign behavior as the power. It starts positive and then undergoes a sign change before becoming zero for $D = 1 = D_f$. The drift term does not become zero when reaching D_f because of the probability distribution around D_f; we have to include values around D_f when calculating the expectation value for the drift term.

The deterministic power and drift terms behave similarly regarding their sign. What might be surprising is that the deterministic power becomes negative before the drift term. This is because, for the drift term, we

have to include values around the expected value when calculating the expectation value. Since the function, $\gamma(D_f - D)\partial_D H(D)$, is not symmetric around zero but instead bigger for negative values, the drift term becomes zero when the expected position of $D(t)$ is positive. On the other hand, the deterministic power already becomes zero when the position of $D(t)$ becomes zero.
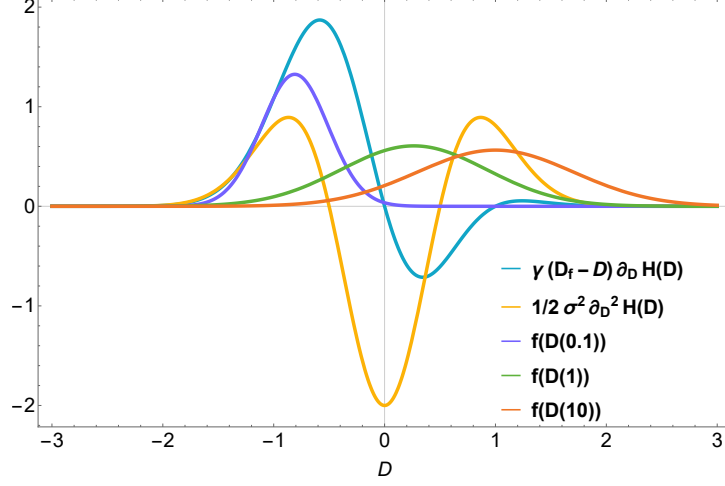

Figure 4: Functions of the drift and diffusion term dependent on the position D without taking the expectation value in light blue and orange. Additionally, we see the probability distribution of $D(t)$ for the times $t = 0.1, 1.0, 10$. When increasing the time, the distribution of $D(t)$ moves to the right with increasing variance. The choice for the parameters here is again $\gamma = 1$, $\sigma = 1$, $\alpha = 2$, $E_0 = 1$, $D_i = -1$ and $D_f = 1$.

We see that the diffusion and drift term become constant at long times because the distribution of the particle's position becomes stable.
For the probability density, this means that it converges to a density with a non-zero variance

$$D(t \to \infty) \sim \mathcal{N}(D_f, \frac{\sigma^2}{2\gamma}). \tag{46}$$

The drift and diffusion terms add up to zero in the limit $t \to \infty$. This means there is always an energy exchange between drift and diffusion terms, or both of them are zero. The limit of both them is

$$\lim_{t \to \infty} \langle \gamma(D_f - D)(-2\alpha E_0 D e^{-\alpha D^2}) \rangle = \lim_{t \to \infty} -\langle \sigma^2 \alpha E_0 e^{-\alpha D^2}(1 - 2\alpha D^2) \rangle$$
$$= \frac{E_0 e^{-\frac{D_f^2 \alpha \gamma}{\gamma + \alpha \sigma^2}} \alpha \sigma^2 \gamma^{3/2}(\gamma - 2D_f^2 \alpha \gamma + \alpha \sigma^2)}{\sqrt{\alpha \sigma^2 + \gamma}(\gamma + \alpha \sigma^2)^2}. \tag{47}$$

This is because the first and second derivative of the Hamiltonian $H(D)$ is non-zero around D_f, which is the point the random process is drifting towards.
On the other hand, we see that the deterministic power turns to zero. This can be seen in Eq. 45 as $D_{det} \to D_f$ the power goes to zero.

There are some interesting limiting cases for $t \to \infty$. For example, in the limit $\sigma \to \infty$ drift, and diffusion terms go to zero. This corresponds to a distribution with infinite variance. Since the first derivative of our Hamiltonian is close to zero everywhere besides close to the origin, this means the drift term turns to zero as $\sigma \to \infty$. The same thing happens in the limit $\gamma \to 0$.

The limit $\gamma \to \infty$ corresponds to a delta peak around D_f for the distribution. Here, the terms converge to

$$\lim_{t, \gamma \to \infty} -\langle \sigma^2 \alpha E_0 e^{-\alpha D^2}(1 - 2\alpha D^2) \rangle = -E_0 e^{-D_f \alpha} \alpha(1 - 2D_f^2 \alpha)\sigma^2. \tag{48}$$

11

We can see that there is a sign change at $D_f^2 \alpha = 1/2$ because the second derivative of the Hamiltonian changes its sign at this point.

The limit $\sigma \to 0$ corresponds to removing all randomness for the process, which results in both the drift and diffusion term going to zero for $t \to \infty$.

$$\lim_{t, \frac{1}{\sigma} \to \infty} -\langle \sigma^2 \alpha E_0 e^{-\alpha D^2} (1 - 2\alpha D^2) \rangle = 0. \tag{49}$$

With the average power for all $t \in [0, \tau]$ we can also calculate the average work in the time-interval $[0, \tau]$. The results of this calculation are illustrated in Fig. 5.
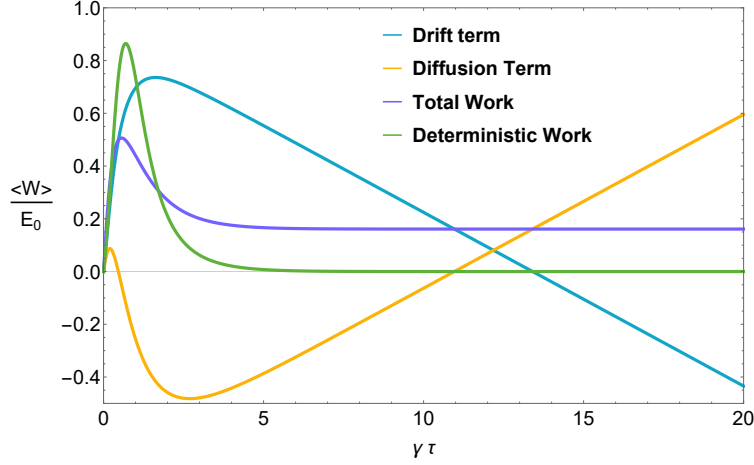

Figure 5: Average work done by the particle in the time interval $[0, \tau]$. Here, we compare the average total work with the work produced in the same process with $\sigma = 0$. Drift and diffusion term refers to the terms in Eq. (42).

We see that the average total work, in contrast to the deterministic work for $\tau \to \infty$, is not zero.

For the deterministic Ornstein Uhlenbeck process in this example, the work done in the interval $[0, \infty]$ is zero since $D_i = -D_f$ and $H(D) = H(-D)$ is symmetric around zero. The particle moves to a position with the same energy it had at the start of its path, corresponding to the total work as shown in Eq. (26). Therefore, the deterministic work for $\tau \to \infty$ is zero.

For the non-deterministic case, the average value of $D(t)$ still goes to D_f as $\tau \to \infty$. For the average work done, we also have to include the probability distribution around said average value according to Eq. (34). Since we start with a delta peak around D_i and end with a normal distribution around D_f with variance $\sigma^2/2\gamma$, the total work turns out to be non-zero.

$$\langle W(\tau) \rangle = \langle H(D(\tau)) - \langle H(D(0)) \rangle \rangle \tag{50}$$

$$= \int_{-\infty}^{\infty} E_0 e^{-\alpha D^2} \frac{1}{\sqrt{V(D)}\sqrt{2\pi}} e^{-\frac{1}{2}\left(\frac{D - \langle D \rangle}{V(D)}\right)^2} dD - E_0 e^{-\alpha D_i^2} \tag{51}$$

$$= E_0 \left(\frac{e^{-\frac{(D_i + D_f(-1 + e^{\tau\gamma}))^2 \alpha\gamma}{-\alpha\sigma^2 + e^{2\tau\gamma}(\gamma + \alpha\sigma^2)}}}{\sqrt{\frac{(1 - e^{-2\tau\gamma})}{\gamma}}\sqrt{\frac{-\alpha\sigma^2 + e^{2\tau\gamma}(\gamma + \alpha\sigma^2)}{(-1 + e^{2\tau\gamma})}}} \right) - E_0 e^{-\alpha D_i^2} \tag{52}$$

$$\xrightarrow{\tau \to \infty} E_0 \left(e^{-\frac{D_f^2 \alpha\gamma}{\gamma + \alpha\sigma^2}} \sqrt{\frac{\gamma}{\gamma + \alpha\sigma^2}} \right) - E_0 e^{-\alpha D_i^2} \neq 0. \tag{53}$$

There are some limits where the total work is zero. $\gamma \to \infty$ or $\sigma \to 0$ correspond to a path with zero average work in the limit $\tau \to \infty$.

We can also check that the result of Sec. 3.2 does hold for this example. The details for this can be found

in App. C.

$$\langle W \rangle = \int_0^\tau \langle P \rangle dt = \langle H(D(\tau)) - \langle H(D(0)) \rangle \rangle. \tag{54}$$

3.3.3 Stochastic case with linear Hamiltonian

In the last chapter, we have seen an example of a process where both drift and diffusion terms do not turn to zero as $t \to \infty$. This was because the first and second derivative of the Hamiltonian $H(D)$ was non-symmetric around D_f, which was the point the random process was drifting towards. Here, we present an example of a system with linear Hamiltonian, which results in a second derivative, which is zero.

In the two quantum toy models we discuss in Sec. 4, we have linear feedback and, therefore, a Hamiltonian that is also linearly dependent on D.

We again look at a particle whose energy depends on its position D.

$$E(D) = E_0 D \equiv H(D). \tag{55}$$

We look at the same Ornstein Uhlenbeck process as in the last chapter. The particle drifts randomly from $D(0) = D_i$ towards D_f following the stochastic differential equation

$$dD = \gamma(D_f - D)dD + \sigma dW. \tag{56}$$

At each time t, the particle's position is normally distributed around its expected position. The average power for each time is the following expression according to Eq. (27)

$$\begin{aligned} \langle P \rangle &= \langle \gamma(D_f - D)\partial_D H(D) \rangle + \frac{1}{2}\langle \sigma^2 \partial_D^2 H(D) \rangle \\ &= \langle \gamma(D_f - D)E_0 \rangle = \gamma E_0(D_f - \langle D \rangle) \\ &= \gamma E_0(D_f - D_i)e^{-\gamma t}. \end{aligned} \tag{57}$$

The deterministic power for a non-random path with $\sigma = 0$ can be calculated with the following.

$$\begin{aligned} P_{det} &= \gamma E_0(D_f - D_{det}(t)) \qquad D_{det}(t) = D_i e^{-\gamma t} + D_f(1 - e^{-\gamma t}), \\ &= \gamma E_0(D_f - D_i)e^{-\gamma t}. \end{aligned} \tag{58}$$

As we can see, the deterministic power is equal to the power in the random process. This is because the random process is normally distributed around its expected position, and the contributions from around the expected position do cancel each other because the derivative of the Hamiltonian is constant.

The average work in the interval $[0, \tau]$ can then be calculated by

$$\begin{aligned} \langle W \rangle &= \int_0^\tau \gamma E_0(D_f - D_i)e^{-\gamma t} dt \\ &= (D_f - D_i)E_0 e^{-\gamma \tau}(e^{\gamma \tau} - 1) \\ &\underset{\tau \to \infty}{\to} E_0(D_f - D_i). \end{aligned} \tag{59}$$

The power and the work in the interval $[0, \tau]$ can also be found in the following plot. As expected, the power turns to zero as $t \to \infty$, and the work becomes constant for $\tau \to \infty$.
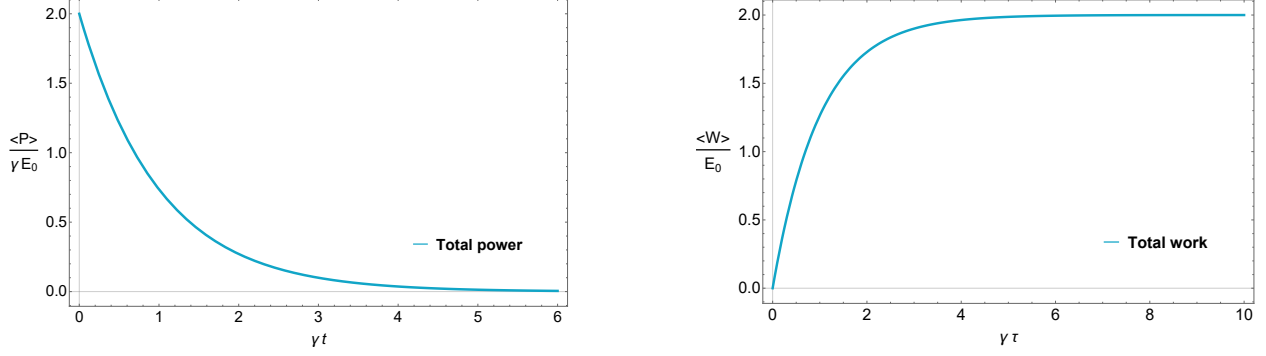
Figure 6: Average power for each time t and average work done by the particle in the time interval $[0, \tau]$. The choice for the parameters here is $\gamma = 1$, $\sigma = 1$, $E_0 = 1$, $D_i = -1$ and $D_f = 1$.

4 Quantum feedback systems

In the following, we will examine two toy models undergoing continuous feedback control in qubits. For such systems, the Fokker-Planck master equation Eq. (12) tells us the time evolution of the joint system and detector state $\hat{\rho}_t(D)$.

Our approach will be to solve the Fokker-Planck master equation for the toy models and then calculate heat, work, and change in measurement energy in the systems.

The goal of this process is to understand what is a suitable approach for solving the Fokker-Planck master equation and to use these simpler toy models to better understand the thermodynamics of quantum systems under feedback control.

4.1 Coherently driven two-level system

The first toy model we discuss is a coherently driven two-level system dependent on the measurement result D of a measurement $\hat{A}$. Such a system can be described by the Hamiltonian

$$\hat{H}(D,t) = \frac{\Delta}{2}\hat{\sigma}_z + gD\frac{i}{2}\left(e^{i\Delta t}\hat{\sigma} - e^{-i\Delta t}\hat{\sigma}^\dagger\right), \qquad \hat{\sigma} = \hat{\sigma}_x + i\hat{\sigma}_y. \tag{60}$$

For weak coupling, $\Delta \gg g$, the energy difference between the ground and excited state is approximately Δ while gD is the drive strength. It is to be noted that the measurement result does change the drive strength continuously through the measurement result D.

This Hamiltonian could, for example, be realized by a spin 1/2-particle in a magnetic field [17] or by light in a cavity coherently driven by a laser [18].

We define our measurement in a rotating frame around the z-axis in the Bloch sphere as $A = \hat{\sigma}_x$. The transformed state $\hat{\chi}_t(D) = \hat{U}(t)\hat{\rho}_t(D)\hat{U}^\dagger(t)$ then follows Eq. (12) with Liouvillian superoperator $\mathcal{L}(D)\hat{\rho}_t(D) = -igD[\hat{\sigma}_y, \hat{\rho}_t(D)]$. Proof of this can be found in the App. D.

In this setup, the ground state is an eigenstate of $\hat{\sigma}_z$ with eigenvalue -1. Suppose we initially prepare the starting state as the ground state. In that case, as we continuously measure $\hat{A} = \hat{\sigma}_x$, the state is dephasing into the eigenbasis of $\hat{\sigma}_x$ due to measurement backaction [1]. This means the measurement puts energy into the system by moving the state away from the ground state.

Counteracting this movement is the Rabi oscillation of the state because of the Hamiltonian $\hat{H} = gD\hat{\sigma}_y$, which would push us back into the starting ground state because of its dependence on the measurement result D. A positive/negative measurement result D means the measured state has a positive/negative x-coordinate in the Bloch sphere. A sign change in D also introduces a sign change in the Hamiltonian, which introduces a Rabi oscillation in the direction that pushes the state back to the ground state.

In the steady state, we expect Rabi oscillation and measurement backaction to cancel each other. Therefore, we expect a distribution close to the ground state for the steady state.

As explained in the introduction Sec. 1, this toy model presented here is the continuous version of a

measurement-driven engine discussed in [8]. Instead of temporally dividing measurement and drive, we let both act on the state simultaneously.

4.1.1 Finding the steady state

As said before, our initial goal is to solve the Fokker-Planck master equation to better understand heat and work in this system. The first step towards that goal was to switch into a rotating frame to simplify the time-dependent Hamiltonian.

The next step is to write the density matrix $\hat{\rho}_t(D)$ as

$$\hat{\rho}_t(D) = \frac{1}{2}\left(P(D,t)\mathbb{1}_2 + b_x(D,t)\hat{\sigma}_x + b_y(D,t)\hat{\sigma}_y + b_z(D,t)\hat{\sigma}_z\right). \tag{61}$$

These new functions represent the coordinates in the Bloch sphere of the quantum state after measuring a certain measurement result D. In more detail $\frac{b_i(D)}{P(D,t)}$ tells us the coordinate on the i-axis for $i = \{x, y, z\}$ after measuring the outcome D. $P(D,t) = \mathrm{Tr}\{\hat{\rho}_t(D)\}$, on the other hand, tells us the probability distribution of the measurement results themselves.

This expression transforms the Fokker-Planck master equation into four coupled differential equations, see App. E for details

$$\partial_t P(D,t) = \gamma\partial_D(DP(D,t) - b_x(D,t)) + \frac{\gamma^2}{8\lambda}\partial_D^2 P(D,t),$$

$$\partial_t b_x(D,t) = 2gD\, b_z(D,t) + \gamma\partial_D(Db_x(D,t) - P(D,t)) + \frac{\gamma^2}{8\lambda}\partial_D^2 b_x(D,t),$$

$$\partial_t b_y(D,t) = -2\lambda b_y(D,t) + \gamma\partial_D(Db_y(D,t)) + \frac{\gamma^2}{8\lambda}\partial_D^2 b_y(D,t),$$

$$\partial_t b_z(D,t) = -2gD\, b_x(D,t) - 2\lambda b_z(D,t) + \gamma\partial_D(Db_z(D,t)) + \frac{\gamma^2}{8\lambda}\partial_D^2 b_z(D,t). \tag{62}$$

In the next step we use the differential operator $\mathcal{J}(\cdot) = \gamma\partial_D(D\,\cdot) + \frac{\gamma^2}{8\lambda}\partial_D(\cdot)$ to simplify the four differential equations. As we are mainly interested in the steady state, we drop the time dependencies and set the left-hand side to zero.

$$0 = \mathcal{J}P(D) - \gamma\partial_D b_x(D),$$
$$0 = 2gDb_z(D) + \mathcal{J}b_x(D) - \gamma\partial_D P(D),$$
$$0 = -2\lambda b_y(D) + \mathcal{J}b_y(D),$$
$$0 = -2gDb_x(D) - 2\lambda b_z(D) + \mathcal{J}b_z(D). \tag{63}$$

Now we introduce the eigenfunctions $G_n(D)$ of the differential operator $\mathcal{J}$.

$$G_n(D) = \frac{1}{\sqrt{2\pi\sigma}}He_n^{[\sigma]}(D)e^{-\frac{D^2}{2\sigma}}, \qquad \mathcal{J}G_n(D) = -\gamma n G_n(D). \tag{64}$$

Here $He_n^{[\sigma]}(D)$ is the generalized Hermite polynomial with variance $\sigma = \frac{\gamma}{8\lambda}$. More details about these functions and proof of their properties can be found in App. F. We now expand the density matrix further using these functions.

$$P(D) = \sum_{n=0}^{\infty} p_n G_n(D), \qquad b_i(D) = \sum_{n=0}^{\infty} b_n^i G_n(D). \tag{65}$$

We use these expansions in Eq. (63) and multiply with $He_m^{[\sigma]}(D)$. Next, we integrate over dD and use that the Hermite polynomials are orthogonal with regard to the weight $\frac{1}{\sqrt{2\pi\sigma}}e^{\frac{-D^2}{2\sigma}}$

$$\int_{-\infty}^{\infty} dD He_n^{[\sigma]}(D)He_m^{[\sigma]}(D)\frac{1}{\sqrt{2\pi\sigma}}e^{\frac{-D^2}{2\sigma}} = \delta_{n,m}n!\sigma^n. \tag{66}$$

After taking the sum over n to get rid of the $\delta_{n,m}$, this leaves us with the following system of linear equations. The full calculation can be found in the App. G

$$0 = mp_m - \frac{1}{\sigma}b^x_{m-1},$$
$$0 = -2\lambda b^y_m - \gamma m b^y_m,$$
$$0 = gb^z_{m-1} + g(m+1)\sigma b^z_{m+1} - \frac{\gamma}{2}mb^x_m + \frac{\gamma}{2\sigma}p_{m-1},$$
$$0 = -gb^x_{m-1} - g(m+1)\sigma b^x_{m+1} - \lambda b^z_m - \frac{\gamma}{2}mb^z_m. \tag{67}$$

Here, all the negative indices are zero by definition. We can see that all $b^y_m = 0$ since both γ and λ are positive constants as they represent the detector bandwidth and the measurement strength. Additionally, conservation of probabilities implies $p_0=1$. The other terms can be determined by solving the linear equations.

Based on the system of linear equations, we can tell which functions of $P(D)$ or $b_i(D)$ are even or odd. To see this, we split the system of linear equations into two smaller independent sets of linear equations

$$0 = 2lp_{2l} - \frac{1}{\sigma}b^x_{2l-1},$$
$$0 = gb^z_{2l} + g(2l+2)\sigma b^z_{2l+2} - \frac{\gamma}{2}(2l+1)b^x_{2l+1} + \frac{\gamma}{2\sigma}p_{2l},$$
$$0 = -gb^x_{2l-1} - g(2l+1)\sigma b^x_{2l+1} - \lambda b^z_{2l} - \frac{\gamma}{2}2lb^z_{2l}. \tag{68}$$

$$0 = (2l+1)p_{2l+1} - \frac{1}{\sigma}b^x_{2l}$$
$$0 = gb^z_{2l-1} + g(2l+1)\sigma b^z_{2l+1} - \frac{\gamma}{2}(2l)b^x_{2l} + \frac{\gamma}{2\sigma}p_{2l-1}$$
$$0 = -gb^x_{2l} - g(2l+2)\sigma b^x_{2l+2} - \lambda b^z_{2l+1} - \frac{\gamma}{2}(2l+1)b^z_{2l+1}. \tag{69}$$

All p_m with m even, b^x_m with m odd, and b^z_m with m even are part of the first set of equations, and all p_m for m odd, b^x_m for m even, and b^z_m for m odd are part of the second set of equations. We immediately see that for the second set of equations, all unknowns being zero is a possible solution. This is also the only possible solution if we have a unique steady state, which we expect in this system.

This means the only nonzero unknowns are p_m for m even, b^x_m for m odd, and b^z_m for m even. These unknowns cannot all be zero since, for the first set of equations, all unknowns being zero is not a solution as $p_0 = 1$. Next, we use the fact that Hermite polynomials are even or odd depending on their degree

$$He^{[\sigma]}_n(-D) = (-1)^n He^{[\sigma]}_n(D). \tag{70}$$

This means $P(D) = \sum p_m G_m(D)$ is an even function of D, $b_x(D)$ is odd, and $b_z(D)$ is even as well. $P(D)$ being an even function makes sense since we expect the steady state to be a distribution around the ground state where positive and negative measurement results are equally likely. $b_z(D)$ is then even, as both the measurement feedback dephasing the state into the eigenbasis of $\hat{\sigma}_x$ and the measurement-controlled rotation around the y-axis is symmetrical for negative/positive measurement results. The same thing goes for the function $b_x(D)$ being odd. When measuring $\hat{\sigma}_x$, if your measurement result is positive/negative, then your state will be closer to the $|+\rangle/|-\rangle$ state respectively, therefore $b_x(D)$ will be positive/negative as well, resulting in an odd function.

The numerical approach to solving the system of equations will be to make a cut-off after the first n linear equations and then numerically solve the resulting system of linear equations, giving us the values for the unknowns p_m, b^i_m. We plot the resulting functions $P(D)$ and $b^i(D)$. The details of this can be found in App. H.

An example of the solution for the steady state can be seen in Fig. 7. The even/odd behavior of the

functions can also be observed. Here $\frac{b_i(D)}{P(D)}$ tells us the coordinate on the i-axis of the system state for $i = \{x, y, z\}$ after measuring the outcome D in the Bloch sphere, and $P(D) = \text{Tr}\{\hat{\rho}_t(D)\}$ tells us the probability distribution of the measurement results themselves.

We introduce the notation $\hat{d}_+, \hat{d}_-$ for the two states of the system after measuring the measurement result D with the highest probability $P(D)$. For some parameter combinations, there is only one measurement result with the highest probability; in that case, these two states overlap.

The system's steady state is a distribution around the ground state with the two most likely measurement outcomes corresponding to the system states $\hat{d}_+$ and $\hat{d}_-$. A stronger measurement would move these states closer to the $|+\rangle/|-\rangle$ states, while a stronger drive with higher bandwidth would move these states closer to the ground state.
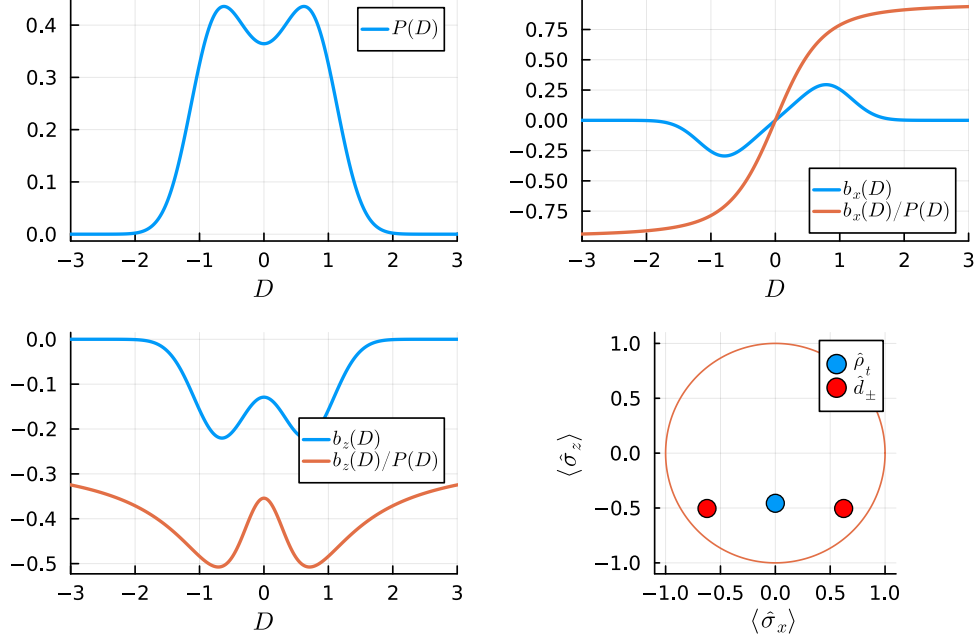

Figure 7: Plot of the steady state for the choice of parameters $g = \lambda = \gamma = 1$. In the first three plots, the functions $P(D), b_i(D)$ can be seen together with the function $b_i(D)/P(D)$, which tells us the value of the i-axis of the system state in the Bloch sphere after measuring the measurement outcome D.

On the bottom right, we see the average system state $\hat{\rho}_t$ for an unknown measurement outcome, and the two system states $\hat{d}_\pm$ we get after measuring the two most likely measurement outcomes in the Bloch sphere. Remember, we always have $b_y(D) = 0$ for this system.

4.1.2 Calculate heat, work, and change in measurement energy

To summarize the last chapter, we find a system of linear equations that, when numerically solved, gives us the unique steady state of the system described by $P(D)$, and $b_i(D)$. Now, we want to calculate the components of the average energy change of the system based on Eq. (14) and Eq. (20).

We change into a rotating frame to find the steady state solution $\hat{\chi}_t(D) = \hat{U}(t)\hat{\rho}_t(D)\hat{U}^\dagger(t)$. We can now calculate the average energy changes outside the rotating frame based on the steady state in the rotating frame. The three main steps in this calculation are inserting identities $\mathbb{1}_2 = \hat{U}(t)\hat{U}^\dagger(t)$ in the right position, using the cyclic property of the trace, and partial integration. The full calculation can be found in the

App. I.

$$\gamma \left\langle \mathcal{A}(D)\partial_D \hat{H}(D,t)\right\rangle_{\mathrm{lab}} = -g\gamma \left\langle D\,\hat{\sigma}_y\right\rangle,$$

$$\lambda \left\langle \mathcal{D}[\hat{A}]\hat{H}(D,t)\right\rangle_{\mathrm{lab}} = -\lambda\left(\Delta\left\langle\hat{\sigma}_z\right\rangle + 2g\left\langle D\,\hat{\sigma}_y\right\rangle\right),$$

$$\left\langle \partial_t \hat{H}(D,t)\right\rangle_{\mathrm{lab}} = -g\Delta\left\langle D\,\hat{\sigma}_x\right\rangle. \tag{71}$$

We used the following notation

$$\left\langle\hat{O}\right\rangle_{\mathrm{lab}} = \int \mathrm{Tr}\{\hat{O}\hat{\rho}_t(D)\}dD, \qquad \left\langle\hat{O}\right\rangle = \int \mathrm{Tr}\{\hat{O}\hat{\chi}_t(D)\}dD. \tag{72}$$

In this system, the diffusion term is zero because of $\partial_D^2 \hat{H}(D) = 0$. In a quantum system without feedback control and no thermal bath, this would mean the drift term would have to be zero as well. However, in a quantum system under feedback control, we have the change in measurement energy through the measurement backaction that puts energy into the system and leads to a nonzero drift term.

This means in this system, power and change in measurement energy are

$$\langle P\rangle = -g(\gamma\left\langle D\,\hat{\sigma}_y\right\rangle - \Delta\sigma\left\langle D\,\hat{\sigma}_x\right\rangle),$$

$$\langle \dot{E}_M\rangle = -\lambda\left(\Delta\left\langle\hat{\sigma}_z\right\rangle + 2g\left\langle D\,\hat{\sigma}_y\right\rangle\right). \tag{73}$$

In the steady state, we use the notation $b_i(D) = \sum b_n^i G_n(D) = \mathrm{Tr}\{\hat{\chi}(D)\hat{\sigma}_i\}$ and find

$$\langle P\rangle = -\langle\dot{E}_M\rangle = \lambda\Delta\langle\hat{\sigma}_z\rangle = \lambda\Delta b_0^z. \tag{74}$$

Again, the calculation can be found in the App. I. We can see $\partial_t\left\langle\hat{H}(D)\right\rangle = 0$ as we expected for the steady state. There is a continuous energy exchange between the measurement energy and work. For positive parameter g, the measurement backaction puts energy into the system, which is then turned into work.

4.1.3 Special case g=0

Before discussing the general solution, we look at a special case where we can solve the Fokker-Planck master equation analytically for the steady state. By setting $g = 0$, we remove the drive and simplify the Hamiltonian in the rotating frame to $\hat{H}(D,t) = 0$. This means the only evolution of the system in the rotating frame stems from the measurement backaction. In this simplified model, there is also no measurement feedback. For $g = 0$, the system of linear equation Eq. (67) does simplify to

$$0 = mp_m - \frac{1}{\sigma}b_{m-1}^x,$$

$$0 = -2\lambda b_m^y - \gamma m b_m^y,$$

$$0 = -\frac{\gamma}{2}m b_m^x + \frac{\gamma}{2\sigma}p_{m-1},$$

$$0 = -\lambda b_m^z - \frac{\gamma}{2}m b_m^z. \tag{75}$$

We directly see that $b_m^y = b_m^z = 0\ \forall m \geq 0$. As in the general system, we again have $p_m = 0$ for m even and $b_m^x = 0$ for m odd. The nonzero unknowns are then

$$p_m = \frac{1}{\sigma^m m!}\ \text{for m even}, \quad b_m^x = \frac{1}{\sigma^m m!}\ \text{for m odd}. \tag{76}$$

We can now use the generating function for the Hermite polynomials $\sum_{m=0}^{\infty}\frac{t^n}{n!}He_n(x) = e^{xt - t^2/2}$ to find the functions $P(D)$, and $b_x(D)$. The details of this calculation can be found in App. J

$$P(D) = \frac{1}{2\sqrt{2\pi\sigma}}\left(e^{-(D-1)^2/2\sigma} + e^{-(D+1)^2/2\sigma}\right),$$

$$b_x(D) = \frac{1}{2\sqrt{2\pi\sigma}}\left(e^{-(D-1)^2/2\sigma} - e^{-(D+1)^2/2\sigma}\right). \tag{77}$$

In Fig. 8, we can see the analytical steady-state solutions for this system. The system states with the highest probability are always the two states $|+\rangle/|-\rangle$. Increasing the measurement strength makes the peaks of $P(D)$ around $D = \pm 1$ narrower; the stronger measurement means there is less variance in the measurement results and, therefore, a lower chance of being in a mixed state. An increase in the bandwidth does the opposite; a wider range of possible measurement results means wider peaks for $P(D)$.
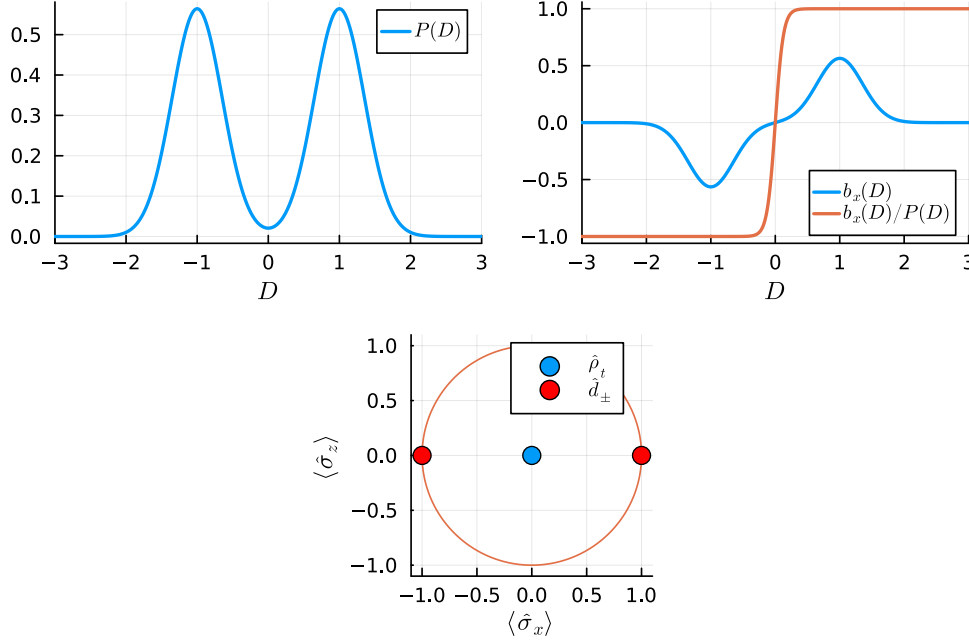

Figure 8: Analytical solution for the system's steady state with $g = 0$. The parameter choice is here $\gamma = \lambda = 1$. We can see that the missing drive means the system is in the eigenbasis of the measurement operator. The function $b_z(D)$ is equal to zero.

Based on Eq. (74), we can also analytically calculate work and change in measurement energy in this system

$$\langle P \rangle = -\langle \dot{E}_M \rangle = \lambda \Delta b_0^z = 0. \tag{78}$$

We removed the drive by setting $g = 0$. Therefore, nothing pushes us out of the eigenbasis of the measurement operator. In the general system, two "forces," the measurement back action and the drive, cancel each other on average in the steady state. These two movements are responsible for the nonzero work and change in measurement energy. Here, the missing drive means both work and change in measurement energy are zero.

4.1.4 Discussion of the heat and change in measurement energy of the general system

Now, after looking at the special case $g = 0$, we discuss the numerically calculated work and change in the average measurement energy of the general system. We plot the work dependent on a parameter for different parameter combinations and then analyze the results. In Fig. 9, we can see the work dependent on the parameter g for some chosen combination of γ, λ values.
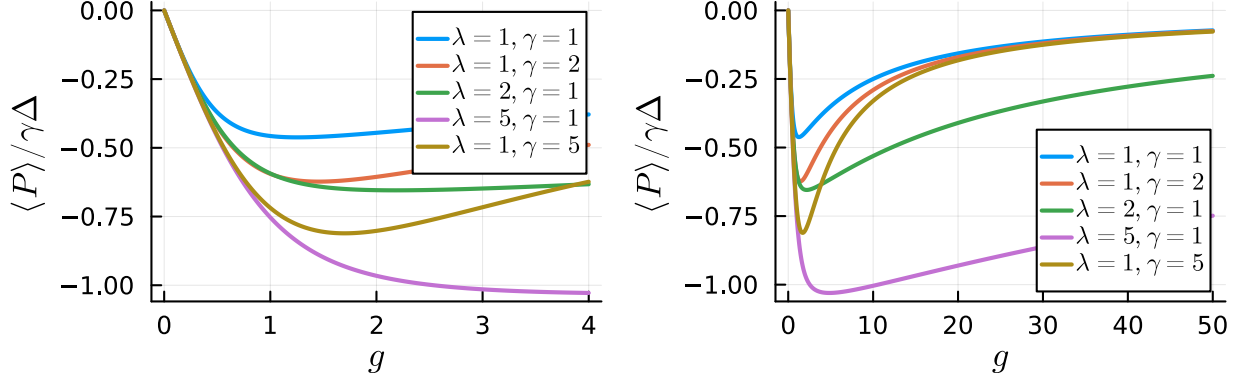
Figure 9: Work dependent as a function of the drive strength g for different values for γ, λ. Here, negative work means positive extracted work. We can see that increasing g first increases the extracted work only up to a certain maximum point. Increasing g further means decreasing the work again. The limit for $g \to \infty$ is zero.

As we can see, increasing the drive strength g does increase the extracted work only up to a certain point, after which the extracted work starts to drop with increasing g. For chosen γ and λ, the work is only dependent on $\langle \hat{\sigma}_z \rangle$. This means the extracted work is maximized when we are, on average, as close to the ground state as possible. Increasing the drive strength g increases the Rabbi-oscillation that pushes us toward the ground state until we start overcorrection our position. Remember the filtered measurement outcome drifts towards a value determined by the system state at a rate that scales with $1/\gamma$. If we make the drive strength too fast, we overshoot the ground state before the filtered measurement changes its sign. For a too-high drive strength, we move towards a maximally mixed state from which no work is extracted. This behavior can be seen in Fig. 10 for the example $\lambda = \gamma = 1$. Increasing the drive strength only moves the average system state down up to a certain point.
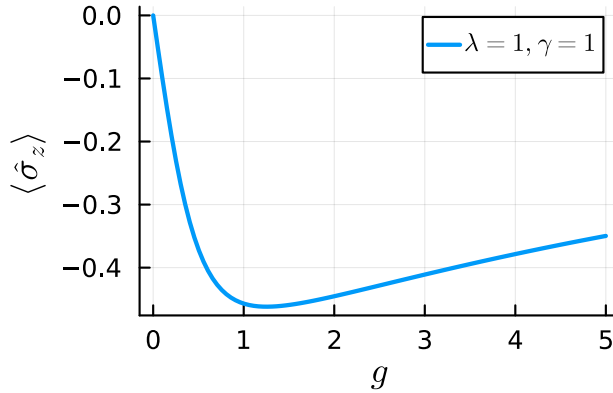

Figure 10: Here, we see the expectation value of the z-coordinate in the Bloch sphere steady state for different drive strengths. Increased drive strength pushes the average system state down toward the ground state. The optimal drive strength for $\gamma = \lambda = 1$ is around $g = 1.25$. As we can see, both lower drive strength and higher drive strength mean lower extracted work.

For the dependence of the extracted work on the measurement strength λ and bandwidth γ in Fig. 11, we find that for both variables, the higher, the more extracted work. For both variables, there is a maximum value for the extracted work in the limit $\gamma, \lambda \to \infty$.
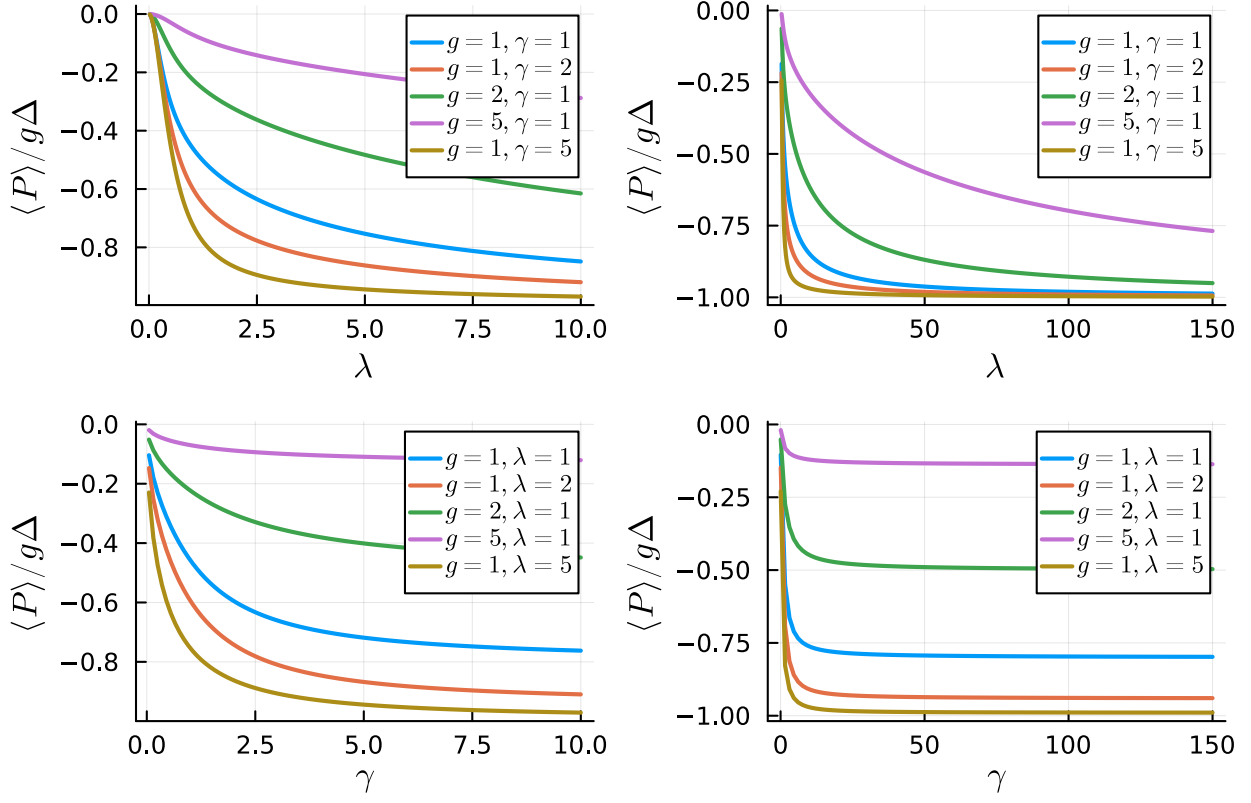
Figure 11: We find that for the dependence of the extracted work on λ and γ when we increase the value of these variables, the extracted work increases as well. For both variables, the extracted work has a maximum value in the limits $\gamma \to \infty$ or $\lambda \to \infty$.

For γ, the behavior can be explained similarly to the behavior with g. Higher bandwidth means the filtered measurement outcome drifts faster toward the value determined by the system. This means the information if we measured a positive or negative measurement outcome is brought faster into the Hamiltonian. That means the drive direction is changed faster when a change in the sign of the measurement outcome happens. On the other hand, high bandwidth introduces more measurement noise. Naively, we could assume that this noise decreases the extracted work, but that does not seem to happen in this system compared to the second system, see Sec. 4.2.5. One possible explanation could be that this noise leads to dephasing, which would be for this system dephasing in y, as seen in Eq. (81). Since both y-eigenstates have the same energy, this does not greatly affect the extracted work. However, this is speculative, and further work is needed to fully explain this behavior in γ. In Sec. 4.1.5, we confirm this behavior of the extracted work for $\gamma \to \infty$.

Higher λ means the measurement strength increases. This means in the rotating frame, we get pushed more strongly into the eigenbasis of $\hat{A}$. For a strong continuous measurement, the system state becomes a mixed state of $|+\rangle$ and $|-\rangle$, the eigenstates of $\hat{\sigma}_x$, with low off-diagonal elements. The energy of a state in these positions gets changed the most by the drive compared to other positions in the Bloch sphere, and therefore, we observe a high extracted work.

This can be illustrated by looking at a state in a two-level system with the constant Hamiltonian $\hat{H} = g\hat{\sigma}_y$ and assuming the time evolution

$$\partial_t \hat{\rho}_t = -i[\hat{H}, \hat{\rho}_t]. \tag{79}$$

In this system, we have

$$\partial_t \langle \hat{\sigma}_x \rangle(t) = 2g\langle \hat{\sigma}_z \rangle(t) = 2g \operatorname{Tr}\{\hat{\sigma}_x \hat{\rho}_t\},$$
$$\partial_t \langle \hat{\sigma}_z \rangle(t) = 2g\langle \hat{\sigma}_x \rangle(t). \tag{80}$$

21

We see that for $\langle\hat{\sigma}_x\rangle(t) = 1$ the z-coordinate of the Bloch sphere $\langle\hat{\sigma}_z\rangle$ changes the fastest which results in a fast energy change since this is measured by $\frac{\Delta}{2}\langle\hat{\sigma}_z\rangle$.

The reason the state in the mixed state of $|+\rangle$ and $|-\rangle$ does not move on average besides being changed the most by the drive is the introduced Zeeno effect because of the strong measurement backaction that continuously moves the state back towards said mixed state. While the Zeno effect keeps us in an eigenstate of σ_x, the power does still not vanish because, as we can see from Eq. (74), the power is boosted by λ. In more detail, $b_0^z = \langle\hat{\sigma}_z\rangle$ vanishes as $1/\lambda$ due to the Zeno effect, but the prefactor compensates for this.

Summarized, we find that the extracted work is maximized for a projective measurement with a large bandwidth while the optimal drive strength g depends on the chosen γ and λ.

This is a similar result to what was found in [8]. In this paper, the extracted work was maximized in the Zeno limit of quickly repeating projective measurements.

4.1.5 Fast detector limit

For the limit $\gamma \to \infty$, according to Eq. (22) we can find a master equation for the system state $\hat{\rho}_t$

$$\partial_t\hat{\rho}_t = -ig[\hat{\sigma}_y, \mathcal{A}\hat{\rho}_t] + \lambda\mathcal{D}[\hat{\sigma}_x]\hat{\rho}_t + \frac{1}{4\lambda}\mathcal{D}[g\hat{\sigma}_y]\hat{\rho}_t. \tag{81}$$

As we can see, the fast detector limit introduces a new term that leads to dephasing into y. We write the system state as

$$\hat{\rho}_t = \frac{1}{2}\left(\mathbb{1} + B_x\hat{\sigma}_x + B_y\hat{\sigma}_y + B_z\hat{\sigma}_z\right), \qquad B_i = \langle\hat{\sigma}_i\rangle = \mathrm{Tr}\{\hat{\sigma}_i\hat{\rho}_t\}. \tag{82}$$

and multiply with $\hat{\sigma}_i$. After taking the trace, this leaves us with three differential equations. Details of the derivation can be found in App. K

$$\partial_t B_x = -\frac{g^2}{2\lambda}B_x,$$
$$\partial_t B_y = -2\lambda B_y,$$
$$\partial_t B_z = -2g - 2\lambda b_z - \frac{g^2}{2\lambda}B_z. \tag{83}$$

This means we find the following solution for the master equation

$$B_x(t) = c_1 e^{-\frac{g^2}{2\lambda}t},$$
$$B_y(t) = c_2 e^{-2\lambda t},$$
$$B_z(t) = c_3 e^{-2\lambda t - \frac{g^2}{2\lambda}t} - \frac{4g\lambda}{g^2 + 4\lambda^2}. \tag{84}$$

Where the starting condition determines c_1, c_2, c_3. One example of the solution when starting in the $+1$ eigenstate of $\hat{\sigma}_x$ can be seen in Fig. 12. We can see that the time-dependent Hamiltonian does what we expect it to do: Pushing the system state down towards the -1 eigenstate of $\hat{\sigma}_z$. The fast detector limit does not influence this behavior.
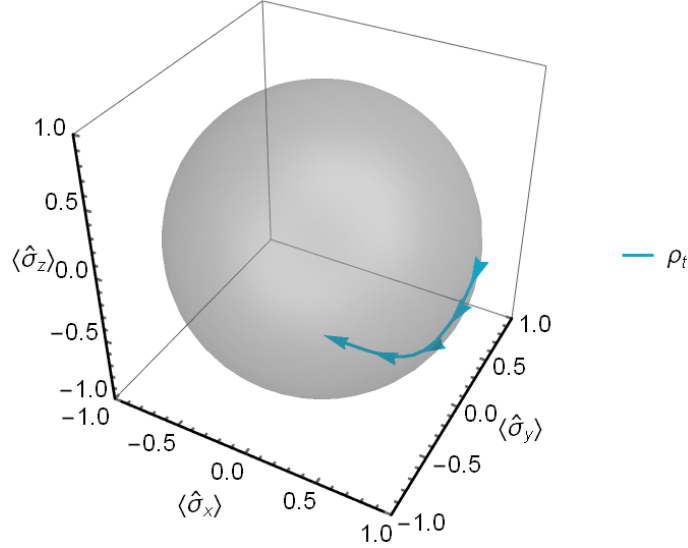
Figure 12: Analytical solution for the system state $\hat{\rho}_t$ in the limit $\gamma \to \infty$ when starting in the $+1$ eigenstate of $\hat{\sigma}_x$ The system is only a pure state for $t = 0$ and moves on a curved line towards the longtime limit on the z-axis with $\langle\hat{\sigma}_z\rangle = -4/5$. For the parameters, $\lambda = g = 1$ was used.

As we can see, the long-time limit and steady state is

$$
\begin{aligned}
B_x(t) &= 0, \\
B_y(t) &= 0, \\
B_z(t) &= -\frac{4g\lambda}{g^2 + 4\lambda^2}.
\end{aligned}
$$
(85)

This result for the steady state is in line with the numerical calculation we did in the non-limit case in Sec. 4.1.1. When increasing γ we numerically find $\langle\hat{\sigma}_z\rangle \approx -\frac{4g\lambda}{g^2+4\lambda^2}$. An example of this can be found in App. L.

We can't calculate the extracted work or change in measurement energy over time; see in Eq. (73). For this calculation, we would need the full information of the detector state, which is included in $\hat{\rho}_t(D)$ but not in the system state $\hat{\rho}_t$.
The information about the detector state is however not needed to calculate the extracted work for the steady state as seen in Eq. (74). This means we find an analytical expression for the extracted work and change in measurement energy in the steady state

$$
\langle P \rangle = -\Delta \frac{4g\lambda^2}{g^2 + 4\lambda^2} = -\langle \dot{E}_M \rangle.
$$
(86)

The behavior of the extracted work is illustrated in Fig. 13. We see that increasing g increases the extracted work up to a certain point, at which point the extracted work declines again. This behavior is equal to the behavior seen in Fig. 9; taking $\gamma \to \infty$ does not change this behavior. Now, with an analytic expression for the extracted work, we can find the point where the extracted work is maximal. We find the maximum by calculating $\partial_g\langle P\rangle=0$, which turns out to be $g = 2\lambda$. This results in a power of $\langle P \rangle = -\lambda\Delta$.
When looking at the behavior when increasing λ, we see that the extracted work increases and converges to $\langle P \rangle = -g\Delta$. This behavior can be seen in Fig. 10 in the bottom right. The higher λ is chosen, the higher the limit of the extracted work for $\gamma \to \infty$, but the limit never increases below $-\Delta g$.
We can see for a projective measurement in the fast detector limit, the extracted work is $\langle P \rangle = -\Delta g$. This means, in theory, that the extracted work can be increased indefinitely.
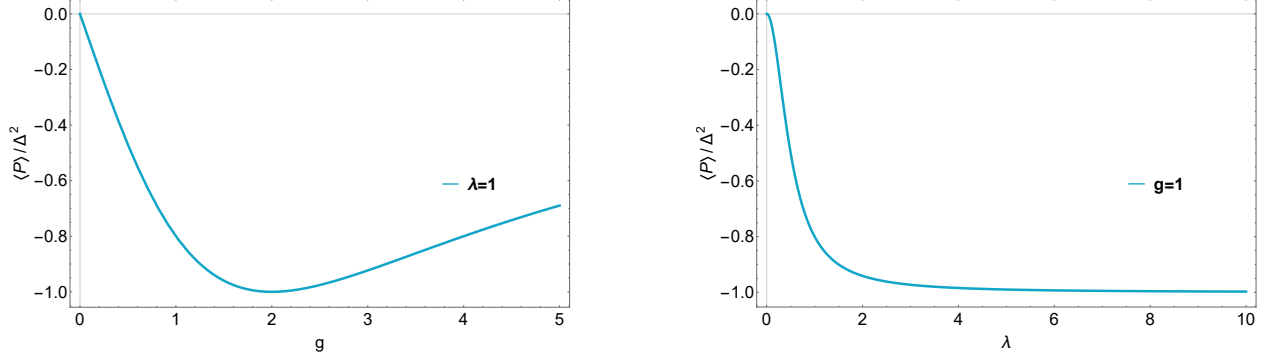
Figure 13: Extracted work in the steady state for the limit $\gamma \to \infty$ for $\Delta = 1$. On the right, we see the extracted work for $g = 1$ dependent on λ, and on the left, we see the extracted work for $\lambda = 1$ dependent on g. Remember, negative work means positive extracted work. The right function converges to $-g = -1$ for $\lambda \to \infty$.

4.2 Two-level system with time-independent Hamiltonian

This second toy model is a continuation of the ideas of the first toy model. Now, instead of using a time-dependent drive that pushes our system state towards the ground state, we rotate the Hamiltonian according to the measurement outcome. The system we discuss is described by the Hamiltonian

$$\hat{H} = -aD\hat{\sigma}_x + b\hat{\sigma}_z. \tag{87}$$

The measurement providing the continuous feedback in our system is $\hat{A} = \hat{\sigma}_x$. The idea behind this choice of Hamiltonian and measurement is that we again expect a distribution around the ground state as our steady-state solution with the difference that now the position of the ground state changes with the measurement outcome.

We measure in the x-basis, which moves the state towards the x-eigenbasis. The Hamiltonian is chosen such that the system state is close to the ground state of the Hamiltonian. When measuring a positive/negative measurement result D, we know that the state has a positive/negative x-coordinate in the Bloch sphere. The "$-$" sign in front of $aD\hat{\sigma}_x$ now ensures that the ground state of the Hamiltonian is close to the system state. One example of this is shown in Fig. 14 in the next section.

For finite b, the ground state is tilted away from the eigenstate of $\hat{\sigma}_x$, resulting in a precession around an axis defined by the Hamiltonian. When starting in an eigenstate of x, this precession brings you into a superposition of both eigenstates. This means a measurement can bring the system state close to the other x-eigenstate, which is higher in energy. This changes the sign of the x-coordinate and, therefore, also changes the sign of the measurement outcome. This sign change then changes the Hamiltonian in such a way that the ground state is again brought close to the system state, which reduces the energy and lets us extract work from the system.

For $b = 0$, the system stays in the x-eigenbasis because the precession introduced by the Hamiltonian is not tilted away from the x-axis. This means for a strong measurement, we simply stay in the ground state of the Hamiltonian.

This system is an example of a measurement-driven engine that does not use a drive Hamiltonian to extract the work. Both increasing the system's energy and the extraction of the work are based on continuous measurement.

4.2.1 Feedback-independent Hamiltonian

Here, we explain some features of the chosen Hamiltonian by visualizing how the Hamiltonian impacts the system. We do this by calculating the evolution of two system states by a static Hamiltonian $\hat{H}(D_f)$ after measuring a certain fixed measurement outcome D_f. Here, we will include no further measurements to simplify. That means the whole evolution of the state is determined by $\hat{H}(D_f)$.

We picked two system states from the steady state solution of the full system with continuous measurement

24

feedback found in Fig. 15. We picked the system states after measuring the most probable measurement outcomes. The two states are marked with red dots in the two top right plots in Fig. 15. They correspond to the measurement outcomes of $D_\pm = \pm 0.87$.

In Fig. 14, we can see the path these two states follow purely on the precession introduced by the fixed Hamiltonian $\hat{H}(D_\pm)$. The calculations of this can be found in App. M.
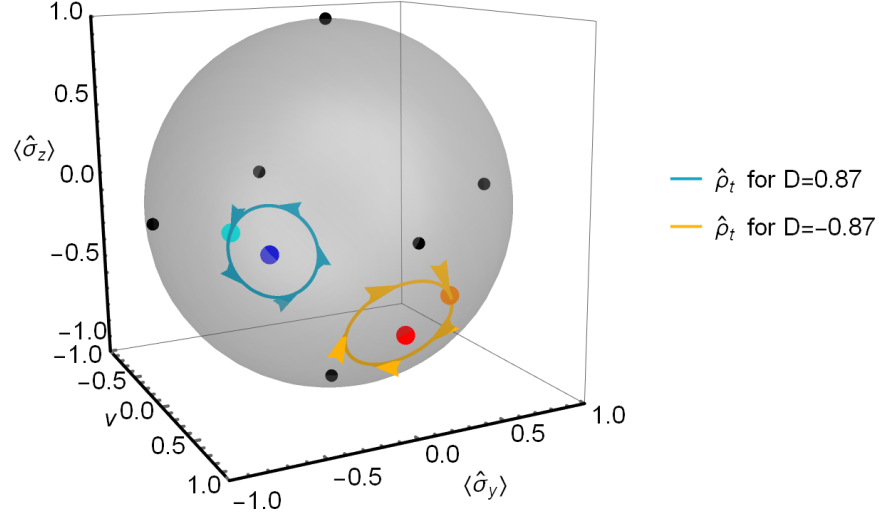

Figure 14: Visualization of the two system states, marked with a cyan and orange dot, after measuring the most probable measurement outcomes in the steady state for $a = 2, \gamma = \lambda = b = 1$. The orange and blue circles represent the precession introduced by the fixed Hamiltonian $H(D_\pm)$. The red and blue dots represent the ground states of the respective Hamiltonian while the black dots show us the eigenstates of $\hat{\sigma}_i$.

This shows us the role of the Hamiltonian of pushing the state away from the eigenstates of $\hat{\sigma}_x$ towards a negative value of $\langle \hat{\sigma}_z \rangle$. We also see that the measurement dependence of the Hamiltonian means that the system state is close to the ground state. This means we are in a state with low energy, which can be increased by jumping close to the other x-eigenstate through a measurement.

4.2.2 Finding the steady state

This process for this toy model is similar to that of the first toy model in Sec. 4.1.1. Therefore, we only present the main steps here.

We again start with the goal of solving the Fokker-Planck master equation Eq. 12, and the first step is again to expand the system state into the function $P(D)$ and $b_i(D)$, see Eq. (61). This leads to the following system of coupled differential equations. See App. E for details.

$$\partial_t P(D,t) = \gamma \partial_D (DP(D,t) - b_x(D,t)) + \frac{\gamma^2}{8\lambda} \partial_D^2 P(D,t),$$

$$\partial_t b_x(D,t) = -2b\, b_y(D,t) + \gamma \partial_D (Db_x(D,t) - P(D,t)) + \frac{\gamma^2}{8\lambda} \partial_D^2 b_x(D,t),$$

$$\partial_t b_y(D,t) = 2aD\, b_z(D,t) + 2bb_x(D,t) - \lambda b_y(D,t) + \gamma \partial_D (Db_y(D,t)) + \frac{\gamma^2}{8\lambda} \partial_D^2 b_y(D,t),$$

$$\partial_t b_z(D,t) = -2aD\, b_y(D,t) - 2\lambda b_z(D,t) + \gamma \partial_D (Db_z(D,t)) + \frac{\gamma^2}{8\lambda} \partial_D^2 b_z(D,t). \tag{88}$$

With the same procedure as in the Seq. 4.1.1, we find the following linear equations for the steady state. The full calculation can be found in the App. G.

$$
\begin{aligned}
0 &= m p_m - \frac{1}{\sigma} b_{m-1}^x, \\
0 &= -b\, b_m^y - \frac{\gamma}{2} m b_m^x + \frac{\gamma}{2\sigma} p_{m-1}, \\
0 &= a\, b_{m-1}^z + a(m+1)\sigma b_{m+1}^z + b\, b_m^x - \lambda b_m^y - \frac{\gamma}{2} m b_m^y, \\
0 &= -a\, b_{m-1}^y - a(m+1)\sigma b_{m+1}^y - \lambda b_m^z - \frac{\gamma}{2} m b_m^z.
\end{aligned}
\tag{89}
$$

This system of linear equations can again be split into two subsystems of linear equations with the following unknowns

$$
\begin{aligned}
\text{First system: } & \{p_{2l}, b_{2l+1}^x, b_{2l+1}^y, b_{2l}^z, \quad \forall l \geq 0\}, \\
\text{Second system: } & \{p_{2l+1}, b_{2l}^x, b_{2l}^y, b_{2l+1}^y, \quad \forall l \geq 0\}.
\end{aligned}
\tag{90}
$$

The second set of equations has the solution of all unknowns being zero. This is the only possible solution for the unique steady state that we expect for this system. All unknowns being zero is not a possible solution for the first system of linear equations as $p_0 = 1$ because of the conservation of probabilities.

This means the only non-zero unknowns are even p_m, odd b_m^x, b_m^y, and even b_m^z. Because Hermite polynomials are even or odd depending on their degree, see Eq. 70; this means that $P(D)$ is even, $b_x(D), b_y(D)$ are odd, and $b_z(D)$ is again even.

The behavior of the functions can partially be explained by the expectation that we find a distribution around the ground state as the steady state. Because positive and negative measurement results are both equally likely $P(D)$ is even. We also measure $\hat{A} = \hat{\sigma}_x$, which means a positive/negative measurement result means positive/negative values for $b_x(D)$, resulting in an odd function. For a non-zero measurement result, for $a \gg b$, the main movement introduced by the Hamiltonian is a precession around the x-axis pushing the system toward the -1 eigenstate of $\hat{\sigma}_z$. This precession changes directions for a sign change in D, making $b_z(D)$ even. This precession around the x-axis also means the average y-coordinate has to be zero in the steady state, which is described by an odd function $b_y(D)$.

We again use a cut-off approach to solve the system of linear equations numerically and plot the resulting function $P(D), b^i(D)$. Details of this can be found in the App. H.

In Fig. 15, we can find one example of the steady-state solution of this system. The system is for this parameter choice distributed around two states close to the $\hat{\sigma}_x$ eigenvalues. Both of these states are close to their respective ground state. The even/odd behavior of the functions can also be observed. We again introduce the notation $\hat{d}_\pm$ for the system states after measuring the measurement results with the highest probability. The states with the highest probability are close to the $|+\rangle / |-\rangle$ states because of the measurement backaction but slightly shifted away by the precession introduced by the Hamiltonian.
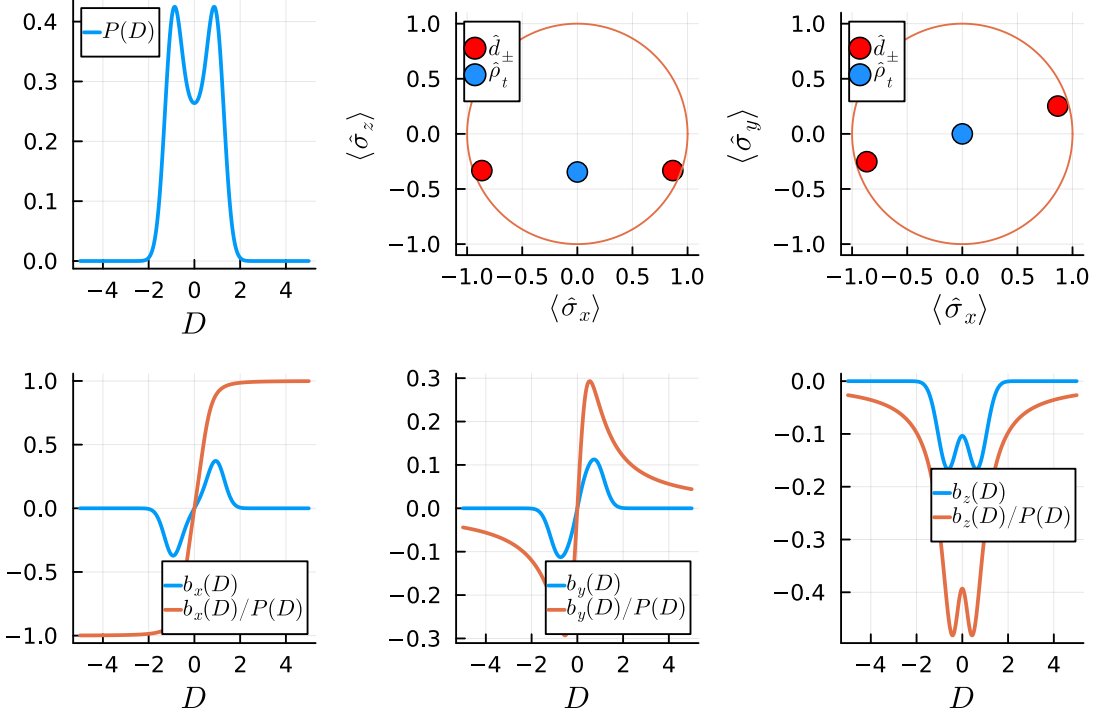
Figure 15: Plots of the functions $P(D), b^i(D)$ and $b_i(D)/P(D)$ for $a = 2, b = 1, \gamma = 1, \lambda = 1$. The two plots on the top right show the average system state as a blue dot and the two system states after measuring the most likely measurement outcome as two red dots. We split the three coordinates into two images to show the full three-dimensional Bloch sphere, showing the x-axis on the bottom.

4.2.3 Calculate heat, work, and change in measurement energy

Based on the found steady state, we can calculate the components of the average energy change. The full calculation can be found in the App. I.

$$\gamma \left\langle \mathcal{A}(D) \partial_D \hat{H}(D) \right\rangle = -\gamma a \left(1 - \sigma \langle D\hat{\sigma}_x \rangle\right),$$
$$\lambda \left\langle \mathcal{D}[\hat{A}] \hat{H}(D) \right\rangle = -2\lambda b \langle \hat{\sigma}_z \rangle. \tag{91}$$

We used the following notation

$$\left\langle \hat{O} \right\rangle = \int \text{Tr}\{\hat{O}\hat{\rho}_t(D)\} dD, \qquad b_i(D) = \sum b_n^i G_n(D) = \text{Tr}\{\hat{\rho}(D)\hat{\sigma}_i\}. \tag{92}$$

Similarly to the last system, the diffusion term is zero, but we have a nonzero drift term. In general, work and change in measurement energy are

$$\langle P \rangle = -\gamma a \left(1 - \sigma \langle D\hat{\sigma}_x \rangle\right),$$
$$\langle \dot{E}_M \rangle = -2\lambda b \langle \hat{\sigma}_z \rangle. \tag{93}$$

In the steady state, we can rewrite these expressions into

$$\langle P \rangle = -\langle \dot{E}_M \rangle = 2\lambda b b_0^z. \tag{94}$$

We can see $\partial_t \left\langle \hat{H}(D) \right\rangle = 0$, as we expected for the steady state. There is a continuous energy exchange between the measurement energy and work. For positive parameter a, the measurement backaction puts

energy into the system, which is then turned into work. For a negative parameter a, the precession introduced by the Hamiltonian pushes the system into the upper half plane of the Bloch sphere, which leads to $\langle \hat{\sigma}_z \rangle > 0$ and, therefore, to negative extracted work.

4.2.4 Special case b=0

In the special case $b = 0$, we can find an analytic solution for the steady state. Setting $b = 0$ means reducing the Hamiltonian to

$$\hat{H}(D) = -aD\,\hat{\sigma}_x. \tag{95}$$

This means the movement produced by the Hamiltonian is a precession around the x-axis with a direction dependent on the measurement result D. In this simple case, the system of linear equations Eq. (89) reduces to

$$0 = mp_m - \frac{1}{\sigma}b^x_{m-1},$$

$$0 = -mb^x_m + \frac{1}{\sigma}p_{m-1},$$

$$0 = a\,b^z_{m-1} + a(m+1)\sigma b^z_{m+1} - \lambda b^y_m - \frac{\gamma}{2}mb^y_m,$$

$$0 = -a\,b^y_{m-1} - a(m+1)\sigma b^y_{m+1} - \lambda b^z_m - \frac{\gamma}{2}mb^z_m. \tag{96}$$

This splits up the top two and bottom two linear equations. The bottom two equations can be solved by setting $b^z_m = b^y_m = 0$. Similar to Seq. 4.1.3, the solution of the top two equations involves setting $p_m = 0$ for m even and $b^x_m = 0$ for m odd. The only non-zero unknowns are then

$$p_m = \frac{1}{\sigma^m m!} \text{ for m odd}, \quad b^x_m = \frac{1}{\sigma^m m!} \text{ for m even.} \tag{97}$$

We can now use the generating function for the Hermite polynomials to find the functions $P(D)$ and $b_x(D)$. The details of this calculation can be found in the App. J

$$P(D) = \frac{1}{2\sqrt{2\pi\sigma}}\left(e^{-(D-1)^2/2\sigma} + e^{-(D+1)^2/2\sigma}\right),$$

$$b_x(D) = \frac{1}{2\sqrt{2\pi\sigma}}\left(e^{-(D-1)^2/2\sigma} - e^{-(D+1)^2/2\sigma}\right). \tag{98}$$

As we can see, the non-zero functions look the same as in Seq. 4.1.3. This stems from the fact that the whole distribution is restricted to the x-axis in the steady state. This means the precession around the x-axis we have in this second Quantum system has no impact on the steady-state solution.

In Fig. 16, we can see the analytical steady-state solutions for this system. The functions behave the same as in Sec. 4.1.3. Increasing the measurement strength makes the peaks of $P(D)$ narrower while making the bandwidth bigger makes them wider. The work and change of measurement energy, see 91, is zero since we set $b = 0$. We are completely in the eigenbasis of the measurement operator, as the precession introduced by the Hamiltonian does not push us out of the x-eigenbasis. This means we stay in one of the two eigenstates of $\hat{\sigma}_x$ and stay there. This means there are no jumps to the other x-eigenstate because we are never in a mixed state. This means there is no extracted work.
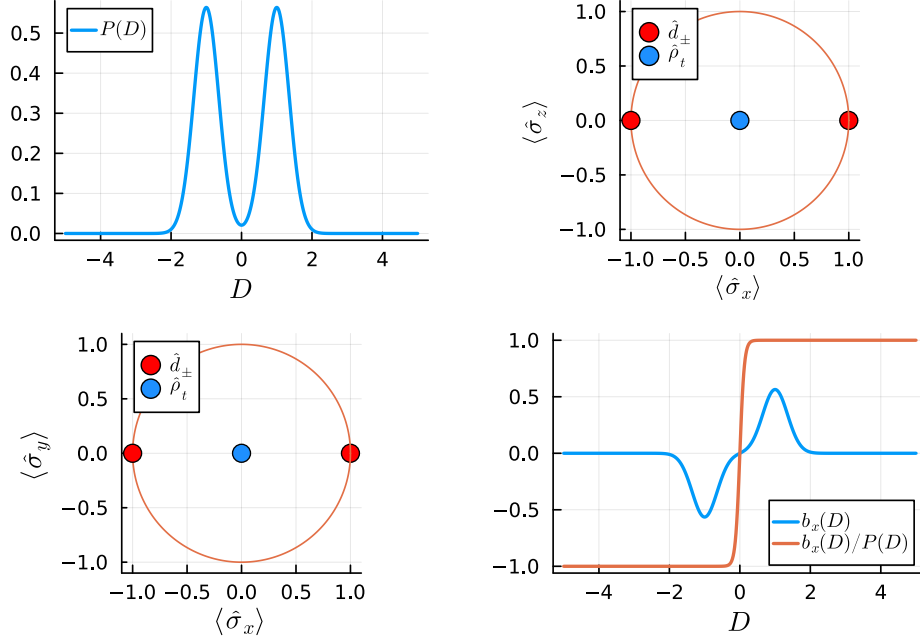
Figure 16: Analytical solution for the steady state of the system with $b = 0$. The parameter choice is here $\gamma = \lambda = 1$. We can see that the missing additional term in the Hamiltonian brings the steady state completely into the eigenbasis of the measurement operator. Remember, both b_y and b_z are zero.

4.2.5 Discussion of the work and change in measurement energy

Now, after looking at the special case $a = 0$, we discuss the numerically calculated work and change in the average measurement energy of the general system. We plot the work dependent on a parameter for different parameter combinations and then analyze the results.

At the start of this section, 4.2, we described how work is extracted from this system. The measurement means we are close to one of the two x-eigenstates in a state with low energy. Because of the precession introduced by the Hamiltonian, we are brought into a superposition of both x-eigenstates, which means we can jump close to the other x-eigenstate through a measurement. This jump increases the energy of the system state. The resulting sign change in the Hamiltonian then brings the ground state close to the system state, decreasing the energy and letting us extract work from the system.

In Fig. 17, we can see the work dependent on the parameters a, b, λ and γ for some chosen parameter combinations.

As we can see, increasing the parameter a does increase the extracted work only up to a certain point, after which the extracted work starts to drop with increasing a further. If the parameter a is too low, the ground state of the Hamiltonian is not moved close to the system state. This means any jump close to the other x-eigenstate does not increase the state's energy, decreasing the extracted work. For a parameter a that is too high, we approach the $b = 0$ limit. We move towards one of the two $\hat{\sigma}_z$ eigenstates and stay there. This means the above-discussed jumps that lead to extracted work become rare.

The parameter b increases the extracted work, but the increase slows down the further one increases the parameter. A high parameter b means the Hamiltonian is independent of the measurement feedback, and only the precession around the z-axis and the measurement feedback remains. This high precession means that the only steady state is the totally mixed state, which we find as the steady state in the limit $b \to \infty$. At the same time, the extracted work is linearly dependent on the parameter b. That means, on the one hand, with increasing b, we move towards a totally mixed state, but on the other hand, the work has a linear dependence on b. These two things seem to cancel each other if b gets big enough and the extracted work

gets constant. One possible explanation might be that a high parameter b means we are pushed out of the x-eigenbasis quickly, increasing jump frequency that leads to extracted work.
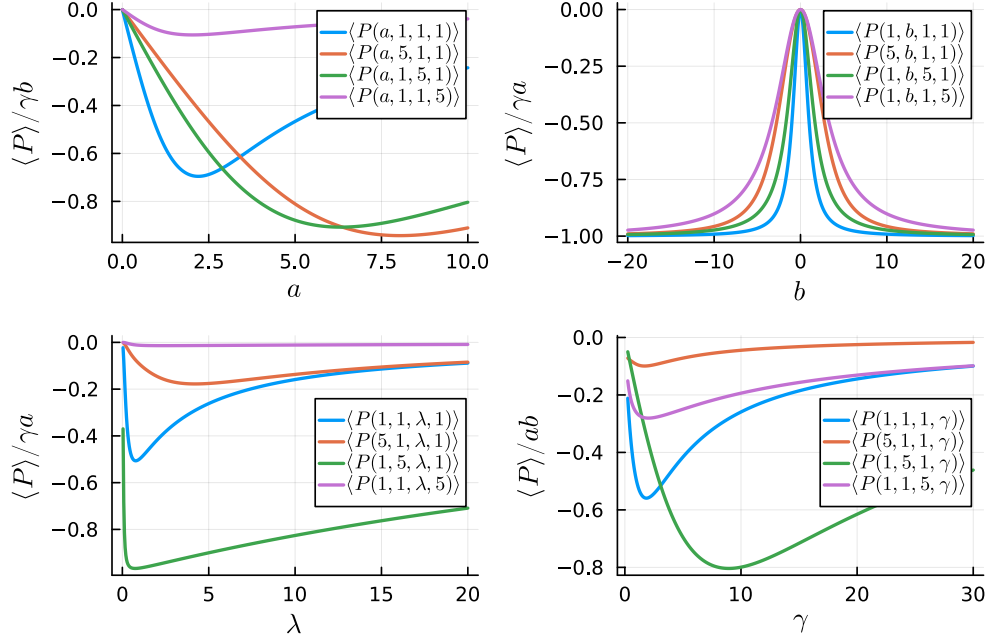

Figure 17: Work dependent on different parameters while the others are fixed. Here, negative work means positive extracted work. We can see that increasing a first increases the extracted work only up to a certain maximum point. Increasing the work further means decreasing the work again. The limit for $a \to \infty$ is zero. Similar behavior can be seen for λ and γ. The behavior for b is different, increasing b does increase the extracted work.

The extracted work dependent on the measurement strength λ does behave similarly to the behavior with the parameter a. First, the extracted work increases but only up to a certain point. Compared to the system in Seq. 4.1, measuring too strong is not a good thing. Because of the Zeno effect, a strong measurement means we are stuck in one of the two x-eigenstates, and the jumps that lead to extracted work do not happen. A very weak measurement is also not great because it corresponds to a high measurement uncertainty. We use the measurement outcome to change the Hamiltonian such that the ground state is close to the system state. Measurement uncertainty makes this process worse, decreasing the extracted work.

The dependence on the bandwidth γ is similar to the dependence on measurement strength. Low bandwidth means the filtered measurement outcome does drift slowly towards the value determined by the system state, which means the ground state is brought slowly close to the system state through the measurement-dependent Hamiltonian. Before this happens, the system state might have already jumped to the other x-eigenstate. Unlike the first system, the bandwidth in this system can be too high; see Sec. 4.1.4. Here, increasing γ too much leads to lower extracted work. This aligns with the naive idea that the higher noise in the measurement leads to lower power output. However, it is unclear why the behavior is different in both systems. One possible explanation might be that this noise leads to dephasing, which would be for this system dephasing in x, as seen in Eq. (99). This can change the energy of the system and can have a large effect on the extracted work. In the first system, it would be dephasing in y, which does not change the energy as much. Further work is needed to fully explain this behavior in γ. In Sec. 4.3, we confirm this behavior of the extracted work in the limit $\gamma \to \infty$.

In summary, this system is more complex than the one with a coherent drive when trying to maximize the extracted energy. The only parameter that can be increased blindly is b; the others have an inverse effect

when increased too far.

4.3 Fast detector limit

For the limit $\gamma \to \infty$, according to Eq. (22) we can find a master equation for the system state $\hat{\rho}_t$

$$\partial_t \hat{\rho}_t = -ib[\hat{\sigma}_z, \hat{\rho}_t] + \left(\lambda + \frac{a}{4\lambda}\right) \mathcal{D}[\hat{\sigma}_x]\hat{\rho}_t. \tag{99}$$

We see the last term introduces a dephasing in x because of the fast detector limit. We again write the system state as

$$\hat{\rho}_t = \frac{1}{2}\left(\mathbb{1} + B_x\hat{\sigma}_x + B_y\hat{\sigma}_y + B_z\hat{\sigma}_z\right), \tag{100}$$

and multiply with $\hat{\sigma}_i$. After taking the trace, this leaves us with three differential equations. Details of the derivation can be found in App. K

$$\partial_t B_x = -2b\, B_y,$$

$$\partial_t B_y = 2b\, B_x - 2\lambda B_y - \frac{a^2}{2\lambda}B_y,$$

$$\partial_t B_z = -2\lambda B_z - \frac{a^2}{2\lambda}B_z. \tag{101}$$

The solution of the master equation then has the following form

$$B_x(t) = e^{-2\lambda t - \frac{a^2}{2\lambda}t}\left(A\sin(Bt) + C\cos(Bt)\right),$$

$$B_y(t) = -e^{-2\lambda t - \frac{a^2}{2\lambda}t}\left(A\sin(Bt) - C\cos(Bt)\right),$$

$$B_z(t) = B_z(0)e^{-2\lambda t - \frac{a^2}{2\lambda}t}. \tag{102}$$

The starting condition and chosen parameters a, b, λ determine A, B, C. As we can see, the system converges for all starting conditions toward the maximally mixed state. This result is in line with our numerical calculation, as seen in App. L.

$$B_x(t) = 0,$$

$$B_y(t) = 0,$$

$$B_z(t) = 0. \tag{103}$$

One example of a system state dependent on time can be found in Fig. 18. We start with $B_i(0) = -1/\sqrt{3}$ and then move in a curved line towards the maximally mixed state.
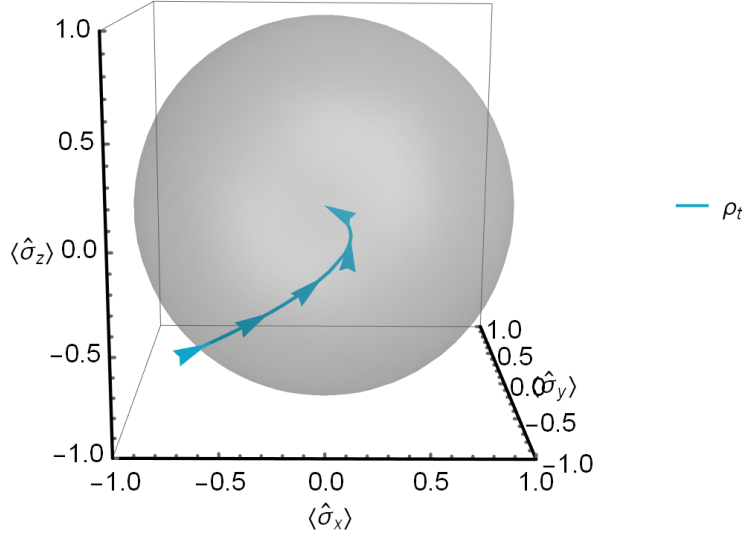
Figure 18: System state dependent on time in the limit $\gamma \to \infty$. The initial state is $B_i(0) = -1/\sqrt{3}$. We can see the long time limit is the maximally mixed state with $B_i = 0$.

Based on Eq. (93), we can see that $\hat{\rho}_t$ is not enough information to calculate the extracted work dependent on time. For this calculation, we would need the full information about the detector only provided by $\hat{\rho}_t(D)$. In the steady state, we can use Eq.(94) and find that the extracted work is zero in the fast detector limit

$$\langle P \rangle = -\langle \dot{E}_M \rangle = 0. \tag{104}$$

This result confirms our result from the last chapter in Sec. 4.2.5. In the fast detector limit, the extracted work turns to zero.

5 Conclusion and Outlook

We explored the thermodynamics of three toy models: One classical model where we used a classical particle to explore heat and work in a randomly evolving system described by a quantum master equation in Sec. 3 and two quantum systems under continuous feedback control in Sec. 4, where we used numerical methods to find their steady-state solutions and then calculated work and change in measurement energy found in Sec. 4.1.4 and Sec. 4.2.5 based on [1] and [10].

In the toy model of the classical particle, found in Sec. 3, we calculated the power and work dependent on time in a system randomly following a path given by an Ornstein-Uhlenbeck process, as seen in Fig. 3 and Fig. 7. We also introduced drift and diffusion terms and discussed their various characteristics and limiting cases as seen, for example, in (47).

The first quantum system was inspired by [8] with the main difference that we used continuous feedback to simultaneously increase the energy of the system via measurement backaction and extract work with a drive Hamiltonian. In this system, we derived a set of linear equations, see (67), to find a steady-state solution for that system. Based on that steady state solution, we derived heat and change in measurement energy as seen in Fig. 9 and Fig. 11 where we discussed the behavior and found ways to optimize the extracted energy, see Sec. 4.1.4. We also included an analytic calculation of the system state in the fast detector limit in Sec. 4.1.5.

The second quantum system is a continuation of the idea of the first, but instead of using a time-dependent drive term, we used a measurement-dependent precession to extract energy from the system. Here, we again derived a system of linear equations, see (89), which, when solved, give us the steady state of the system and calculated heat and change in measurement energy as seen in Fig. 17. Again, we discussed how to optimize the extracted work, as seen in Sec. 4.2.5, and provided an analytic calculation of the fast detector limit in Sec. 4.3.

We found that both quantum toy models we discussed in Sec. 4 are suitable examples of measurement-driven engines. The inclusion of continuous measurement feedback means it is possible to extract work from a system without using a time-dependent drive Hamiltonian.

Our approach also showed a way of finding numerical steady-state solutions of the quantum Fokker-Planck master equation of a system under continuous feedback control. This approach can be generalized to find numerical solutions to the density operator $\hat{\rho}_t(D)$. These numerical solutions make it possible to calculate work, heat, and changes in measurement energy in these systems.

Now, with a way of finding solutions to the quantum Fokker-Planck master equation, the next step would be to couple a thermal bath to one of the two quantum systems we discussed to investigate how this changes extracted work and change in measurement energy. This would create a combination of a measurement-driven and a thermally-driven engine where we could investigate how both these concepts interact with each other. There are also open questions regarding the fast detector limit where we do not fully understand the reason behind the different behaviors of both quantum systems we discussed. Investigating the limit would help us learn more about continuous feedback control and how the bandwidth influences the system's behavior.

References

[1] B. Annby-Andersson, F. Bakhshinezhad, D. Bhattacharyya, G. De Sousa, C. Jarzynski, P. Samuelsson, and P. P. Potts, "Quantum Fokker-Planck master equation for continuous feedback control," *Phys. Rev. Lett.*, vol. 129, p. 050401, Jul 2022. [Online]. Available: https://link.aps.org/doi/10.1103/PhysRevLett.129.050401

[2] S. Vinjanampathy and J. Anders, "Quantum thermodynamics," *Contemporary Physics*, vol. 57, no. 4, pp. 545–579, 2016. [Online]. Available: https://doi.org/10.1080/00107514.2016.1201896

[3] H. M. Wiseman and G. J. Milburn, "Quantum theory of optical feedback via homodyne detection," *Phys. Rev. Lett.*, vol. 70, pp. 548–551, Feb 1993. [Online]. Available: https://link.aps.org/doi/10.1103/PhysRevLett.70.548

[4] V. P. Belavkin, "Quantum stochastic calculus and quantum nonlinear filtering," *Journal of Multivariate Analysis*, vol. 42, no. 2, pp. 171–201, 1992. [Online]. Available: https://www.sciencedirect.com/science/article/pii/0047259X9290042E

[5] K. Maruyama, F. Nori, and V. Vedral, "Colloquium: The physics of Maxwell's demon and information," *Rev. Mod. Phys.*, vol. 81, pp. 1–23, Jan 2009. [Online]. Available: https://link.aps.org/doi/10.1103/RevModPhys.81.1

[6] T. Sagawa and M. Ueda, "Second Law of Thermodynamics with Discrete Quantum Feedback Control," *Phys. Rev. Lett.*, vol. 100, p. 080403, Feb 2008. [Online]. Available: https://link.aps.org/doi/10.1103/PhysRevLett.100.080403

[7] K. Abdelkhalek, Y. Nakata, and D. Reeb, "Fundamental energy cost for quantum measurement," 2018. [Online]. Available: https://arxiv.org/abs/1609.06981

[8] C. Elouard, D. Herrera-Martí, B. Huard, and A. Auffèves, "Extracting Work from Quantum Measurement in Maxwell's Demon Engines," *Phys. Rev. Lett.*, vol. 118, p. 260603, Jun 2017. [Online]. Available: https://link.aps.org/doi/10.1103/PhysRevLett.118.260603

[9] M. C. Cyril Elouard, David A. Herrera-Martí and A. Auffèves, "The role of quantum measurement in stochastic thermodynamics," *npj Quantum Information*, March 2017. [Online]. Available: https://www.nature.com/articles/s41534-017-0008-4#citeas

[10] P. Potts and J. Aschwanden, "The thermodynamics of continuous feedback control," *Project thesis*, 2022. [Online]. Available: https://qtd.physik.unibas.ch/en/publications/

[11] C. A. Brasil, F. F. Fanchini, and R. de Jesus Napolitano, "A simple derivation of the Lindblad equation," *Revista Brasileira de Ensino de Fisica*, vol. 35, no. 1, pp. 01–09, mar 2013. [Online]. Available: https://doi.org/10.1590%2Fs1806-11172013000100003

[12] L. M. Sander, "Kurt Jacobs: Stochastic Processes for Physicists," *Journal of Statistical Physics*, 2012. [Online]. Available: https://doi.org/10.1007/s10955-012-0419-8

[13] M. Sarovar, C. Ahn, K. Jacobs, and G. J. Milburn, "Practical scheme for error control using feedback," *Phys. Rev. A*, vol. 69, p. 052324, May 2004. [Online]. Available: https://link.aps.org/doi/10.1103/PhysRevA.69.052324

[14] C. W. Gardiner, *Handbook of stochastic methods for physics, chemistry and the natural sciences*, 3rd ed., ser. Springer Series in Synergetics. Berlin: Springer-Verlag, 2004, vol. 13. [Online]. Available: https://link.springer.com/book/9783540707127

[15] V. P. Belavkin, "Nondemolition measurements, nonlinear filtering and dynamic programming of quantum stochastic processes," in *Modeling and Control of Systems*, A. Blaquiére, Ed. Berlin, Heidelberg: Springer Berlin Heidelberg, 1989, pp. 245–265. [Online]. Available: https://link.springer.com/chapter/10.1007/BFb0041197

[16] H. M. Wiseman and G. J. Milburn, "Quantum theory of optical feedback via homodyne detection," *Phys. Rev. Lett.*, vol. 70, pp. 548–551, Feb 1993. [Online]. Available: https://link.aps.org/doi/10.1103/PhysRevLett.70.548

[17] R. P. Feynman, R. B. Leighton, and M. Sands, *The Feynman lectures on physics: The Definitive Edition (Vol. 3)*. Pearson, 2009. [Online]. Available: http://www.worldcat.org/isbn/9788131721704

[18] M. O. Scully and M. S. Zubairy, *Quantum Optics*. Cambridge University Press, 1997. [Online]. Available: https://www.cambridge.org/core/books/quantum-optics/08DC53888452CBC6CDC0FD8A1A1A4DD7

A Derivation of the Fokker-Planck equation for a stochastic differential equation

In this section, we derive the Fokker-Planck equation Eq. (31) based on [12]. We start with an arbitrary stochastic differential equation

$$dD = A(D,t)dt + B(D,t)dW. \tag{105}$$

Now let $h(D)$ be an arbitrary function. Using Ito's rule the stochastic differential equation for $h(D)$ is

$$dh = \frac{dh}{dD}A(D,t)dt + \frac{d^2h}{dD^2}\frac{B^2(D,t)}{2}dt + \frac{dh}{dD}B(D,t)dW. \tag{106}$$

Now, taking the average on both sides gives us a differential equation for the mean of h

$$\frac{d\langle h\rangle}{dt} = \left\langle A(D,t)\frac{dh}{dD}\right\rangle + \left\langle \frac{B^2(D,t)}{2}\frac{d^2h}{dD^2}\right\rangle \tag{107}$$

$$= \int_{-\infty}^{\infty}\left(A(D,t)\frac{dh}{dD} + \frac{B^2(D,t)}{2}\frac{d^2h}{dD^2}\right)F(D,t)dD \tag{108}$$

$$= \int_{-\infty}^{\infty}h(D)\left(-\frac{\partial}{\partial D}(A(D,t)F(D,t)) + \frac{1}{2}\frac{\partial^2}{\partial D^2}(B^2(D,t)F(D,t))\right)dD. \tag{109}$$

where in the last step, we did integrate by parts and used that $\lim_{D\to\pm\infty} F(D,t) = 0$.

Alternatively, we can also calculate the derivative of the mean of h by

$$\frac{d}{dt}\langle h\rangle = \frac{d}{dt}\int_{-\infty}^{\infty}h(D)F(D,t)dD = \int_{-\infty}^{\infty}h(D)\frac{\partial}{\partial t}F(D,t)dD. \tag{110}$$

Comparing (107) and (110) and using the fact that both equations must hold for any function $h(D)$ gives us

$$\frac{\partial}{\partial t}F(D,t) = -\frac{\partial}{\partial D}(A(D,t)F(D,t)) + \frac{1}{2}\frac{\partial^2}{\partial D^2}(B^2(D,t)F(D,t)). \tag{111}$$

B Derivation of expectation value and variance of Ornstein-Uhlenbeck process

In this section, we calculate the probability distribution of an Ornstein Uhlenbeck process [12].

$$dD(t) = \gamma(D_f - D)dt + \sigma dW. \tag{112}$$

The first step for solving this stochastic differential equation is the substitution $Y(t) \equiv D(t)e^{\gamma t}$. Now, following Ito's formula, we get

$$dY(t) = \gamma D(t)e^{\gamma t} + e^{\gamma t}dD(t) \tag{113}$$

$$= \gamma D(t)e^{\gamma t} + e^{\gamma t}(\gamma(D_f - D_t)dt + \sigma dW) \tag{114}$$

$$= \gamma D_f e^{\gamma t} + \sigma e^{\gamma t}dW. \tag{115}$$

Now, the right-hand side does not depend on D_t. Therefore, we can integrate both sides to get Y_t and with re-substitution D_t

$$Y(t) = Y(0) + \gamma\int_0^t D_f e^{\gamma s}ds + \sigma\int_0^t e^{\gamma s}dW_s \tag{116}$$

$$= Y(0) + D_f(e^{\gamma t} - 1) + \sigma\int_0^t e^{\gamma s}dW_s \tag{117}$$

$$\Rightarrow D(t) = D_i e^{-\gamma t} + D_f(1 - e^{-\gamma t}) + \sigma\int_0^t e^{\gamma(s-t)}dW_s. \tag{118}$$

We now switch to discrete time steps for the rest of this calculation by defining $\Delta t = t/N$

$$D(t) = \lim_{N \to \infty} D(N\Delta t) = \lim_{N \to \infty} \left(D_i e^{-\gamma N \Delta t} + D_f (1 - e^{-\gamma N \Delta t}) + \sigma \sum_{n=0}^{N-1} e^{\gamma(n\Delta t - t)} \Delta W_n \right) \tag{119}$$

Here, ΔW_n is the Wiener increment of the nth time-step. Now, the stochastic integral on the right side turns into a sum of Gaussian random variables, and therefore it is a Gaussian random variable itself. This means we now know that $D(t)$ is normally distributed, and what is left to calculate is the mean and variance. The average of each single Wiener increment is zero; therefore, the average of $D(t)$ is

$$\langle D(t) \rangle = D_i e^{-\gamma t} + D_f (1 - e^{-\gamma t}). \tag{120}$$

The first two terms do not contribute to the variance because they are not random. The variance of each Wiener increment is Δt, and if we multiply a random variable with a constant c, the variance increases by c^2. This means the variance is

$$V(D(t)) = \lim_{N \to \infty} \sum_{n=0}^{N-1} \sigma^2 e^{\gamma 2(n\Delta t - t)} \Delta t \tag{121}$$

$$= \sigma^2 e^{-2\gamma t} \int_0^t e^{2\gamma s} ds = \frac{\sigma^2}{2\gamma}(1 - e^{-2\gamma t}) \tag{122}$$

C   Calculation of the average work

When calculating the average work using (42), we get terms that are too big to integrate non-numerically.

$$\langle W(t) \rangle = \int_0^t \langle P(s) \rangle ds \tag{123}$$

$$\int_0^t \frac{\sqrt{2} e^{-\frac{D_i + D_f(-1 + e^{\gamma t})^2 \alpha \gamma}{-\alpha\sigma^2 + e^{2\gamma s}(\gamma + \alpha\sigma^2)}} \alpha\gamma(-2D_f(D_f - D_i)e^{\gamma s}\alpha\gamma\sigma^2\alpha\sigma^2 - 2D_f(D_f - D_i)e^{3\gamma s}\gamma(\gamma + \alpha\sigma^2) + e^{2\gamma s}(2(D_f - D_i)^2\gamma^2 + (-1 + 2(2D_f^2 - 2D_f D_i + D_i^2)\alpha)\gamma\sigma^2 - \alpha\sigma^4))}{\sqrt{\frac{(1 - e^{-2\gamma s})\sigma^2}{\gamma}}(\alpha\sigma^2 - e^{2\gamma s}(\gamma + \alpha\sigma^2))^2 \sqrt{\frac{\gamma + 2\alpha\sigma^2 + \gamma \coth \gamma s}{\sigma^2}}} ds.$$

Instead, we show the equality in Eq.(54) by first considering the work done in the time interval $[0, \tau]$ for $\tau = 0$. For the time interval $[0, 0]$ both expressions have to be zero

$$\langle W \rangle = \int_0^0 \langle P(s) \rangle ds = 0 = \langle H(D(0)) \rangle - \langle (H(D(0)) \rangle. \tag{124}$$

Therefore, both expressions are equal for $\tau = 0$. This means at one time both expressions are equal. This means by checking if their derivative is equal as well we have shown that they are equal for all times. This means we now have

$$\int_0^t \langle P(s) \rangle ds = \langle H(D(t)) \rangle - \langle (H(D(0)) \rangle \iff \langle P(t) \rangle = \frac{d}{dt} \langle H(D(t)) \rangle. \tag{125}$$

The right condition can now be checked by direct calculation to conclude that both expressions are equal. This turns out to be the case.

D   Proof of the Fokker-Planck master equation in a rotating frame

In chapter 4.1, we claimed that to get the Fokker-Planck master equation in the rotating frame for the state $\hat{\chi}_t(D) = \hat{U}(t)\hat{\rho}_t(D)\hat{U}^\dagger(t)$ we need to make the following replacements

$$\hat{H}(D,t) \to \hat{U}(t)\hat{H}(D,t)\hat{U}^\dagger(t) - i\hat{U}(t)\partial_t \hat{U}^\dagger(t) = gD\hat{\sigma}_y,$$

$$\hat{A} \to \hat{U}(t)\hat{A}\hat{U}^\dagger(t) = \hat{\sigma}_x, \qquad \hat{U}(t) = e^{-\frac{i\Delta t}{2}\hat{\sigma}_z}. \tag{126}$$

Here, we show that based on the initial Fokker-Planck master equation for $\hat{\rho}_t(D)$ the state in the rotated frame $\hat{\chi}_t(D)$ follows the same Fokker-Planck master equation but with the above replacements.

$$
\begin{aligned}
\partial_t \hat{\chi}_t(D) =\ & \partial_t \hat{U}(t) \hat{\rho}_t(D) \hat{U}^\dagger(t) + \hat{U}(t) \partial_t \hat{\rho}_t(D) \hat{U}^\dagger(t) + \hat{U}(t) \hat{\rho}_t(D) \partial_t \hat{U}^\dagger(t) \\
=\ & -i\hat{U}(t)[\hat{H}(D,t), \hat{\rho}_t(D)]\hat{U}^\dagger(t) + \lambda \hat{U}(t) \hat{A} \hat{\rho}_t(D) \hat{A}^\dagger \hat{U}^\dagger(t) - \frac{1}{2} \hat{U}(t)\{\hat{A}^\dagger \hat{A}, \hat{\rho}_t(D)\} \hat{U}^\dagger(t) \\
& - \gamma \hat{U}(t) \partial_D \frac{1}{2}\{\hat{A} - D, \hat{\rho}_t(D)\} \hat{U}^\dagger(t) + \frac{\gamma^2}{8\lambda} \hat{U}(t) \partial_D^2 \hat{\rho}_t(D) \hat{U}^\dagger(t) + \partial_t \hat{U}(t) \hat{\rho}_t(D) \hat{U}^\dagger(t) + \hat{U}(t) \hat{\rho}_t(D) \partial_t \hat{U}^\dagger(t) \\
=\ & -i[\hat{U}\hat{H}\hat{U}^\dagger, \hat{U}\hat{\rho}_t\hat{U}^\dagger] + \lambda \mathcal{D}[\hat{U}\hat{A}\hat{U}^\dagger]\hat{U}\hat{\rho}_t\hat{U}^\dagger - \gamma\partial_D \frac{1}{2}\{\hat{U}\hat{A}\hat{U}^\dagger - D, \hat{U}\hat{\rho}_t\hat{U}^\dagger\} + \frac{\gamma^2}{8\lambda} \partial_D^2 \hat{U}\hat{\rho}_t\hat{U}^\dagger \\
& + \partial_t \hat{U}\hat{\rho}_t\hat{U}^\dagger + \hat{U}\hat{\rho}_t\hat{U}^\dagger \hat{U}\partial_t\hat{U}^\dagger \quad\quad\quad\quad\quad\quad\quad\quad\quad\quad\quad\quad (127)
\end{aligned}
$$

As a next step, we use the fact that

$$
\partial_t \hat{U} = -\frac{i\Delta t}{2}\hat{\sigma}_z \hat{U} = -\hat{U}\frac{i\Delta t}{2}\hat{\sigma}_z \hat{U}^\dagger \hat{U} = -\hat{U}\partial_t \hat{U}^\dagger \hat{U}. \quad\quad\quad (128)
$$

This means

$$
\partial_t \hat{U}\hat{\rho}_t\hat{U}^\dagger + \hat{U}\hat{\rho}_t\hat{U}^\dagger \hat{U}\partial_t\hat{U}^\dagger = -\hat{U}\partial_t\hat{U}^\dagger\hat{U}\hat{\rho}_t\hat{U}^\dagger + \hat{U}\hat{\rho}_t\hat{U}^\dagger\hat{U}\partial_t\hat{U}^\dagger = -i[-i\hat{U}\partial_t\hat{U}^\dagger, \hat{\rho}_t]. \quad (129)
$$

This concludes our proof, as combining this with our previous calculation means that the state in the rotating frame fulfills the initial Fokker-Planck master equation with the stated substitutions.

$$
\partial_t \hat{\chi}_t(D) = -i[\hat{U}\hat{H}\hat{U}^\dagger - i\hat{U}\partial_t\hat{U}^\dagger, \hat{U}\hat{\rho}_t\hat{U}^\dagger] + \lambda\mathcal{D}[\hat{U}\hat{A}\hat{U}^\dagger]\hat{U}\hat{\rho}_t\hat{U}^\dagger - \gamma\partial_D\frac{1}{2}\{\hat{U}\hat{A}\hat{U}^\dagger - D, \hat{U}\hat{\rho}_t\hat{U}^\dagger\} + \frac{\gamma^2}{8\lambda}\partial_D^2\hat{U}\hat{\rho}_t\hat{U}^\dagger. \quad (130)
$$

E   Derivation of the four coupled differential equations

In this chapter, we derive the four coupled differential equations Eq. (62) and Eq. (88) we use for our two quantum models under feedback control.

Instead of doing two calculations, we combine both systems by writing the Hamiltonian and measurement operator as

$$
\hat{H}(D,t) = X(D,t)\hat{\sigma}_x + Y(D,t)\hat{\sigma}_y + Z(D,t)\hat{\sigma}_z, \quad\quad \hat{A} = a\hat{\sigma}_x + b\hat{\sigma}_y + c\hat{\sigma}_z \quad\quad (131)
$$

We also write the density matrix $\hat{\rho}_t(D)$ as

$$
\hat{\rho}_t(D) = \frac{1}{2}\left(P(D,t)\mathbb{1}_2 + b_x(D,t)\hat{\sigma}_x + b_y(D,t)\hat{\sigma}_y + b_z(D,t)\hat{\sigma}_z\right). \quad\quad (132)
$$

The Fokker-Planck master equation Eq. (12) then has four terms. Here, the Liouvillian superoperator is just $\mathcal{L}(D)\hat{\rho}_t(D) = -i[\hat{H}(D,t), \hat{\rho}_t(D)]$ since we do not include a bath in the two systems.

$$
\partial_t \hat{\rho}_t(D) = -i[\hat{H}(D,t), \hat{\rho}_t(D)] + \lambda\mathcal{D}[\hat{A}]\hat{\rho}_t(D) - \gamma\partial_D\mathcal{A}(D)\hat{\rho}_t(D) + \frac{\gamma^2}{8\lambda}\partial_D^2\hat{\rho}_t(D). \quad\quad (133)
$$

In the following, we calculate the four terms of the Fokker-Planck master equation. We remove the D and t dependencies to keep the equations shorter.

$$
\begin{aligned}
-i[\hat{H}(D,t), \hat{\rho}_t(D)] =\ & -iX\left(\frac{P}{2}[\hat{\sigma}_x, \mathbb{1}] + \frac{b_x}{2}[\hat{\sigma}_x, \hat{\sigma}_x] + \frac{b_y}{2}[\hat{\sigma}_x, \hat{\sigma}_y] + \frac{b_z}{2}[\hat{\sigma}_x, \hat{\sigma}_z]\right) \\
& -iY\left(\frac{P}{2}[\hat{\sigma}_y, \mathbb{1}] + \frac{b_x}{2}[\hat{\sigma}_y, \hat{\sigma}_x] + \frac{b_y}{2}[\hat{\sigma}_y, \hat{\sigma}_y] + \frac{b_z}{2}[\hat{\sigma}_y, \hat{\sigma}_z]\right) \\
& -iZ\left(\frac{P}{2}[\hat{\sigma}_z, \mathbb{1}] + \frac{b_x}{2}[\hat{\sigma}_z, \hat{\sigma}_x] + \frac{b_y}{2}[\hat{\sigma}_z, \hat{\sigma}_y] + \frac{b_z}{2}[\hat{\sigma}_z, \hat{\sigma}_z]\right) \\
=\ & X(D,t)(b_y(D,t)\hat{\sigma}_z - b_z(D,t)\hat{\sigma}_y + Y(D,t)(b_z(D,t)\hat{\sigma}_x - b_x(D,t)\hat{\sigma}_z) \\
& + Z(D,t)(b_x(D,t)\hat{\sigma}_y - b_y(D,t)\hat{\sigma}_x). \quad\quad\quad\quad\quad\quad\quad\quad\quad\quad (134)
\end{aligned}
$$

$$\lambda \mathcal{D}[\hat{A}]\hat{\rho}_t(D) = \lambda \left(\hat{A}\hat{\rho}_t(D)\hat{A} - \frac{1}{2}\{\mathbb{1}, \hat{\rho}_t(D)\} \right)$$

$$= \lambda \left(a^2(\frac{P}{2}\mathbb{1} + \frac{b_x}{2}\hat{\sigma}_x\hat{\sigma}_x\hat{\sigma}_x + \frac{b_y}{2}\hat{\sigma}_x\hat{\sigma}_y\hat{\sigma}_x + \frac{b_z}{2}\hat{\sigma}_x\hat{\sigma}_z\hat{\sigma}_x) \right.$$

$$+ b^2(\frac{P}{2}\mathbb{1} + \frac{b_x}{2}\hat{\sigma}_y\hat{\sigma}_x\hat{\sigma}_y + \frac{b_y}{2}\hat{\sigma}_y\hat{\sigma}_y\hat{\sigma}_y + \frac{b_z}{2}\hat{\sigma}_y\hat{\sigma}_z\hat{\sigma}_y)$$

$$\left. + c^2(\frac{P}{2}\mathbb{1} + \frac{b_x}{2}\hat{\sigma}_z\hat{\sigma}_x\hat{\sigma}_z + \frac{b_y}{2}\hat{\sigma}_z\hat{\sigma}_y\hat{\sigma}_z + \frac{b_z}{2}\hat{\sigma}_z\hat{\sigma}_z\hat{\sigma}_z) \right)$$

$$- \left(\frac{P}{2}\mathbb{1} + \frac{b_x}{2}\hat{\sigma}_x + \frac{b_y}{2}\hat{\sigma}_y + \frac{b_z}{2}\hat{\sigma}_z \right)$$

$$= \frac{\lambda}{2} \left((a^2 + b^2 + c^2 - 1)P(D,t)\mathbb{1} + (a^2 - b^2 - c^2 - 1)b_x(D,t)\hat{\sigma}_x \right.$$

$$\left. + (-a^2 + b^2 - c^2 - 1)b_y(D,t)\hat{\sigma}_y + (-a^2 - b^2 + c^2 - 1)b_z(D,t)\hat{\sigma}_z \right). \tag{135}$$

$$-\gamma\partial_D \mathcal{A}(D)\hat{\rho}_t(D)0 = -\gamma\partial_D \frac{1}{2}\{\hat{A} - D, \hat{\rho}_t(D)\}$$

$$= -\gamma\partial_D \left(\frac{1}{2}\{-D, \hat{\rho}_t(D)\} + a\{\hat{\sigma}_x, \hat{\rho}_t(D)\} + b\{\hat{\sigma}_y, \hat{\rho}_t(D)\} + c\{\hat{\sigma}_z, \hat{\rho}_t(D)\} \right)$$

$$= -\frac{\gamma}{2}\partial_D \left(-2D\hat{\rho}_t(D) + \frac{a}{2}(\{\hat{\sigma}_x, \mathbb{1}\}P + \{\hat{\sigma}_x, \hat{\sigma}_x\}b_x + \{\hat{\sigma}_x, \hat{\sigma}_y\}b_y + \{\hat{\sigma}_x, \hat{\sigma}_z\}b_z) \right.$$

$$+ \frac{b}{2}(\{\hat{\sigma}_y, \mathbb{1}\}P + \{\hat{\sigma}_y, \hat{\sigma}_x\}b_x + \{\hat{\sigma}_y, \hat{\sigma}_y\}b_y + \{\hat{\sigma}_y, \hat{\sigma}_z\}b_z)$$

$$\left. + \frac{c}{2}(\{\hat{\sigma}_z, \mathbb{1}\}P + \{\hat{\sigma}_z, \hat{\sigma}_x\}b_x + \{\hat{\sigma}_z, \hat{\sigma}_y\}b_y + \{\hat{\sigma}_z, \hat{\sigma}_z\}b_z) \right)$$

$$= -\frac{\gamma}{2}\partial_D \left(-2D\hat{\rho}_t(D) + a(P(D,t)\hat{\sigma}_x + b_x(D,t)\mathbb{1}) + b(P(D,t)\hat{\sigma}_y + b_y(D,t)\mathbb{1} \right.$$

$$\left. + c(P(D,t)\hat{\sigma}_z + b_z(D,t)\mathbb{1}) \right). \tag{136}$$

$$\frac{\gamma^2}{8\lambda}\partial_D^2 \hat{\rho}_t(D) = \frac{\gamma^2}{8\lambda}\partial_D^2 \left(\frac{1}{2}(P(D,t)\mathbb{1}_2 + b_x(D,t)\hat{\sigma}_x + b_y(D,t)\hat{\sigma}_y + b_z(D,t)\hat{\sigma}_z) \right). \tag{137}$$

Now, multiplying with Pauli matrices and taking the Trace gives us the following four coupled differential equations for $P(D,t)$ and $b_i(D,t)$.

$$\partial_t P = \lambda(a^2 + b^2 + c^2 - 1)P + \gamma\partial_D(DP + ab_x - bb_y - cb_z) + \frac{\gamma^2}{8\lambda}\partial_D^2 P,$$

$$\partial_t b_x = -2Zb_y + 2Yb_z + \lambda(a^2 - b^2 - c^2 - 1)b_x + \gamma\partial_D(Db_x - aP) + \frac{\gamma^2}{8\lambda}\partial_D^2 b_x,$$

$$\partial_t b_y = 2Zb_x - 2Xb_z + \lambda(-a^2 + b^2 - c^2 - 1)b_y + \gamma\partial_D(Db_y - bP) + \frac{\gamma^2}{8\lambda}\partial_D^2 b_y,$$

$$\partial_t b_z = -2Yb_z + 2Xb_y + \lambda(-a^2 - b^2 + c^2 - 1)b_z + \gamma\partial_D(Db_z - cP) + \frac{\gamma^2}{8\lambda}\partial_D^2 b_z. \tag{138}$$

Now, for example, for the Hamiltonian $H(D) = gD\hat{\sigma}_y$ we set $Y(D,t) = gD, X = Z = 0$, and find the coupled differential equations for that system.

F   Derivation of relations for the generalized Hermite polynomials

Instead of the standard physicists' Hermite polynomials H_n or probabilist's Hermite polynomials He_n, we are using generalized Hermite polynomials $He_n^{[\sigma]}$ with variance σ

$$He_n^{[\sigma]}(x) = \left(\frac{\sigma}{2}\right)^{n/2} H_n\left(\frac{x}{\sqrt{2\sigma}}\right). \tag{139}$$

These generalized Hermite polynomials satisfy the following identity, which means they are an Appell sequence. Here we use in the second step that the physicists' Hermite polynomials are an Appell sequence as well, fulfilling $\partial_x H_n(x) = 2nH_{n-1}(x)$

$$
\begin{aligned}
\partial_x He_n^{[\sigma]}(x) &= \left(\frac{\sigma}{2}\right)^{n/2} \frac{1}{\sqrt{2\sigma}} \partial_x H_n \left(\frac{x}{\sqrt{2\sigma}}\right) \\
&= \left(\frac{\sigma}{2}\right)^{n/2} \frac{1}{\sqrt{2\sigma}} 2n H_{n-1} \left(\frac{x}{\sqrt{2\sigma}}\right) \\
&= \left(\frac{\sigma}{2}\right)^{(n-1)/2} H_{n-1} \left(\frac{x}{\sqrt{2\sigma}}\right) \left(\frac{\sigma}{2}\right)^{1/2} \frac{1}{\sqrt{2\sigma}} 2n \\
&= \left(\frac{\sigma}{2}\right)^{(n-1)/2} H_{n-1} \left(\frac{x}{\sqrt{2\sigma}}\right) n \\
&= n He_{n-1}^{[\sigma]}(x).
\end{aligned}
\tag{140}
$$

They also satisfy a similar recurrence relation as the physicists' Hermite polynomials $H_{n+1}(x) = 2xH_n(x) - \partial_x H_{n-1}(x)$.

$$
\begin{aligned}
He_{n+1}^{[\sigma]}(x) &= \left(\frac{\sigma}{2}\right)^{(n+1)/2} H_{n+1} \left(\frac{x}{\sqrt{2\sigma}}\right) \\
&= \left(\frac{\sigma}{2}\right)^{n/2} \left(\frac{\sigma}{2}\right)^{1/2} \left(2\frac{x}{\sqrt{2\sigma}} H_n \left(\frac{x}{\sqrt{2\sigma}}\right) - \partial_x H_{n-1} \left(\frac{x}{\sqrt{2\sigma}}\right)\right) \\
&= \left(\frac{\sigma}{2}\right)^{1/2} \frac{\sqrt{2}}{\sqrt{\sigma}} x \left(\frac{\sigma}{2}\right)^{n/2} H_n \left(\frac{x}{\sqrt{2\sigma}}\right) - \left(\frac{\sigma}{2}\right)^{1/2} \frac{\sqrt{2\sigma}}{\sqrt{2\sigma}} \left(\frac{\sigma}{2}\right)^{n/2} \partial_x H_{n-1} \left(\frac{x}{\sqrt{2\sigma}}\right) \\
&= x He_n^{[\sigma]}(x) - \sigma \partial_x He_{n-1}^{[\sigma]}(x).
\end{aligned}
\tag{141}
$$

We can also show that the orthonormality of the generalized Hermite polynomials follows from the orthonormality of the physicists' Hermite polynomials using substitution

$$
\begin{aligned}
\int_{-\infty}^{\infty} He_n^{[\sigma]}(x) He_m^{[\sigma]}(x) \frac{e^{-\frac{x^2}{2\sigma}}}{\sqrt{2\pi\sigma}} dx &= \int_{-\infty}^{\infty} \left(\frac{\sigma}{2}\right)^{\frac{n+m}{2}} H_n \left(\frac{x}{\sqrt{2\sigma}}\right) H_m \left(\frac{x}{\sqrt{2\sigma}}\right) \frac{e^{-\frac{x^2}{2\sigma}}}{\sqrt{2\pi\sigma}} dx \\
&= \int_{-\infty}^{\infty} \left(\frac{\sigma}{2}\right)^{\frac{n+m}{2}} H_n(x) H_m(x) \frac{e^{-x^2}}{\sqrt{\pi}} dx \\
&= \delta_{n,m} n! \sigma^n.
\end{aligned}
\tag{142}
$$

In Seq. 4, we frequently use the following function

$$
G_n(D) = \frac{1}{\sqrt{2\pi\sigma}} He_n^{[\sigma]}(D) e^{-\frac{D^2}{2\sigma}}.
\tag{143}
$$

These $G_n(D)$ fulfill the following identity.

$$
\begin{aligned}
\partial_D G_n(D) &= \partial_D \frac{1}{\sqrt{2\pi\sigma}} He_n^{[\sigma]}(D) e^{-\frac{D^2}{2\sigma}} \\
&= \frac{1}{\sqrt{2\pi\sigma}} \left(-\frac{D}{\sigma} e^{-\frac{D^2}{2\sigma}} He_n^{[\sigma]}(D) + \partial_D He_n^{[\sigma]}(D) e^{-\frac{D^2}{2\sigma}}\right) \\
&= -\frac{1}{\sigma} \left(\frac{1}{\sqrt{2\pi\sigma}} e^{-\frac{D^2}{2\sigma}} \left(D He_n^{[\sigma]}(D) - \sigma He_n^{[\sigma]}(D)\right)\right) \\
&= -\frac{1}{\sigma} G_{n+1}(D).
\end{aligned}
\tag{144}
$$

The reason for using the functions $G_n(D)$ is that they are Eigenfunctions of the differential operator $\mathcal{J} = \gamma\partial_D + \gamma\sigma\partial_D^2$ that is part of the differential equations Eq. (62) and Eq. (88).

$$
\begin{aligned}
\mathcal{J}G_n(D) &= (\gamma\partial_D + \gamma\sigma\partial_D^2)\frac{1}{\sqrt{2\pi\sigma}}He_n^{[\sigma]}(D)e^{-\frac{D^2}{2\sigma}} \\
&= \gamma\partial_D\left(\frac{1}{\sqrt{2\pi\sigma}}He_n^{[\sigma]}(D)e^{-\frac{D^2}{2\sigma}}\right) + \gamma\sigma\partial_D\left(\frac{1}{\sqrt{2\pi\sigma}}\partial_D He_n^{[\sigma]}(D)e^{-\frac{D^2}{2\sigma}} - \frac{D}{\sigma}\frac{1}{\sqrt{2\pi\sigma}}He_n^{[\sigma]}(D)e^{-\frac{D^2}{2\sigma}}\right) \\
&= \gamma\sigma\partial_D\left(\frac{1}{\sqrt{2\pi\sigma}}He_n^{[\sigma]}(D)e^{-\frac{D^2}{2\sigma}}\right) \\
&= \gamma\sigma\frac{1}{\sqrt{2\pi\sigma}}e^{-\frac{D^2}{2\sigma}}\left(-\frac{D}{\sigma}\partial_D He_n^{[\sigma]}(D) + \partial_D^2 He_n^{[\sigma]}(D)\right) \\
&= -\gamma\frac{1}{\sqrt{2\pi\sigma}}e^{-\frac{D^2}{2\sigma}}n\left(DHe_{n-1}^{[\sigma]}(D) - \sigma\partial_D He_{n-1}^{[\sigma]}(D)\right) \\
&= -\gamma n G_n(D).
\end{aligned}
\tag{145}
$$

G   Details to the derivation of the system of linear equations for the steady state

In this chapter, we derive the two recurrence relations Eq. 67 and Eq. 89, based on the Fokker-Planck master equation for the systems we look at in chapter Sec. 4.

G.1   Derivation for the first system

After rewriting the four coupled differential equations for the first system Eq. 62 using the $\mathcal{J}$ differential operator, we are left with the following differential equations.

$$
0 = \frac{1}{2}\mathcal{J}P(D) - \frac{\gamma}{2}\partial_D b_x(D),
\tag{146}
$$

$$
0 = gDb_z(D) + \frac{1}{2}\mathcal{J}b_x(D) - \frac{\gamma}{2}\partial_D P(D),
\tag{147}
$$

$$
0 = -\lambda b_y(D) + \frac{1}{2}\mathcal{J}b_y(D),
\tag{148}
$$

$$
0 = -gDb_x(D) - \lambda b_z(D) + \frac{1}{2}\mathcal{J}b_z(D).
\tag{149}
$$

In the following, we go over the calculation of the four recurrence relations in order. We use the new expression for $b_x(D), b_y(D), b_z(D)$ and $P(D)$, see Eq. (61), multiply with $He_m^{[\sigma]}(D)$ and Integrate with respect to D.

$$
\begin{aligned}
0 &= \frac{1}{2}\mathcal{J}P(D) - \frac{\gamma}{2}\partial_D b_x(D) \\
&= -\frac{\gamma}{2}\sum_{n=0}^{\infty}p_n\int dD\, nG_n(D)He_m^{[\sigma]}(D) - \frac{\gamma}{2}\sum_{n=0}^{\infty}b_n^x\int dD\,\partial_D G_n(D)He_m^{[\sigma]}(D) \\
&= -\frac{\gamma}{2}\sum_{n=0}^{\infty}p_n\int dD\, nG_n(D)He_m^{[\sigma]}(D) + \frac{\gamma}{2}\sum_{n=0}^{\infty}b_n^x\int dD\,\frac{1}{\sigma}G_{n+1}(D)He_m^{[\sigma]}(D) \\
&= -\frac{\gamma}{2}\sum_{n=0}^{\infty}p_n\delta_{n,m}n!\sigma^n + \frac{\gamma}{2\sigma}\sum_{n=0}^{\infty}b_n^x\delta_{n+1,m}(n+1)!\sigma^{n+1} \\
&= mp_m\sigma^m m! - \frac{1}{\sigma}m!\sigma^m b_{m-1}^x \\
&= mp_m - \frac{1}{\sigma}b_{m-1}^x.
\end{aligned}
\tag{150}
$$

In the second step, we used Eq. 144; in the third step, we used Eq. 142 to eliminate the integrals. We will also use these two identities for the rest of the calculations here.

$$
\begin{aligned}
0 =\ & gDb_z(D) + \frac{1}{2}\mathcal{J}b_x(D) - \frac{\gamma}{2}\partial_D P(D) \\
=\ & g\sum_{n=0}^{\infty} b_n^z \int dD\, DG_n(D)He_m^{[\sigma]}(D) - \frac{\gamma}{2}\sum_{n=0}^{\infty} b_n^x \int dD\, nG_n(D)He_m^{[\sigma]}(D) - \frac{\gamma}{2}\sum_{n=0}^{\infty} p_n \int dD\, \partial_D G_n(D)He_m^{[\sigma]}(D) \\
=\ & g\sum_{n=0}^{\infty} b_n^z \int dD\, (G_{n+1}(D) + \sigma nG_{n-1}(D))He_m^{[\sigma]}(D) - \frac{\gamma}{2}mb_m^x \sigma^m m! + \frac{\gamma}{2\sigma}m!\sigma^m p_{m-1} \\
=\ & g\sum_{n=0}^{\infty} b_n^z (\delta_{n+1,m}(n+1)!\sigma^{n+1} + \delta_{n-1,m}n!\sigma^n) - \frac{\gamma}{2}mb_m^x \sigma^m m! + \frac{\gamma}{2\sigma}m!\sigma^m p_{m-1} \\
=\ & gb_{m-1}^z \sigma^m m! + g(m+1)!\sigma^{m+1}b_{m+1}^y - \frac{\gamma}{2}mb_m^x \sigma^m m! + \frac{\gamma}{2\sigma}m!\sigma^m p_{m-1} \\
=\ & gb_{m-1}^z + g(m+1)\sigma b_{m+1}^y - \frac{\gamma}{2}mb_m^x + \frac{\gamma}{2\sigma}p_{m-1}.
\end{aligned}
\tag{151}
$$

Observe that the second and third terms appeared similarly in Eq. (150).

$$
\begin{aligned}
0 =\ & -\lambda b_y(D) + \frac{1}{2}\mathcal{J}b_y(D) \\
=\ & -\lambda\sum_{n=0}^{\infty} b_n^y \int dD\, G_n(D)He_m^{[\sigma]}(D) + \frac{\gamma}{2}\sum_{n=0}^{\infty} nb_n^y \delta_{n,m}n!\sigma^n \\
=\ & -\lambda b_m^y m!\sigma^m - \frac{\gamma}{2}b_m^y mm!\sigma^m \\
=\ & -\lambda b_m^z - \frac{\gamma}{2}mb_m^z
\end{aligned}
\tag{152}
$$

Here, we used Eq. (141) in the third line to remove the $D \cdot G_n(D)$. The fourth equation is almost equal to the third with one less term

$$
\begin{aligned}
0 =\ & -gDb_x(D) - \lambda b_z(D) + \frac{1}{2}\mathcal{J}b_z(D) \\
=\ & -g\sum_{n=0}^{\infty} b_n^y \int dD\, DG_n(D)He_m^{[\sigma]}(D) - \lambda b_m^z m!\sigma^m - \frac{\gamma}{2}b_m^z mm!\sigma^m \\
=\ & -g\sum_{n=0}^{\infty} b_n^y (\delta_{n+1,m}(n+1)!\sigma^{n+1} + \delta_{n-1,m}n!\sigma^n) - \lambda b_m^z m!\sigma^m - \frac{\gamma}{2}b_m^z mm!\sigma^m \\
=\ & -gb_{m-1}^y - g(m+1)\sigma b_{m+1}^y - \lambda b_m^z - \frac{\gamma}{2}mb_m^z
\end{aligned}
\tag{153}
$$

G.2 Derivation for the second system

After rewriting the four coupled differential equations for the second system Eq. 88 using the $\mathcal{J}$ differential operator, we are left with the following differential equations.

$$
0 = \frac{1}{2}\mathcal{J}P(D) - \frac{\gamma}{2}\partial_D b_x(D),
\tag{154}
$$

$$
0 = -bb_y(D) + \frac{1}{2}\mathcal{J}b_x(D) - \frac{\gamma}{2}\partial_D P(D),
\tag{155}
$$

$$
0 = aDb_z(D) + bb_x(D) - \lambda b_y(D) + \frac{1}{2}\mathcal{J}b_y(D),
\tag{156}
$$

$$
0 = -aDb_y(D) - \lambda b_z(D) + \frac{1}{2}\mathcal{J}b_z(D).
\tag{157}
$$

In the following, we go over the calculation of the four recurrence relations in order. We again use the new expression of $b_x(D), b_y(D), b_z(D)$ and $P(D)$, see Eq. (61), multiply with $He_m^{[\sigma]}(D)$ and Integrate with respect

to D.

For the first line, see Eq. 150. The differential equation and resulting equation are the same.

$$0 = -bb_y(D) + \frac{1}{2}\mathcal{J}b_x(D) - \frac{\gamma}{2}\partial_D P(D)$$

$$= -b\sum_{n=0}^{\infty} b_n^y \int dD\, G_n(D)He_m^{[\sigma]}(D) - \frac{\gamma}{2}\sum_{n=0}^{\infty} nb_n^x \delta_{n,m} n!\sigma^n + \frac{\gamma}{2\sigma}\sum_{n=0}^{\infty} p_n \delta_{n+1,m}(n+1)!\sigma^{n+1}$$

$$= -b\sum_{n=0}^{\infty} b_n^y \delta_{n,m} n!\sigma^n - \frac{\gamma}{2}\sum_{n=0}^{\infty} nb_n^x \delta_{n,m} n!\sigma^n + \frac{\gamma}{2\sigma}\sum_{n=0}^{\infty} p_n \delta_{n+1,m}(n+1)!\sigma^{n+1}$$

$$= -bb_m^y - \frac{\gamma}{2}b_m^x + \frac{\gamma}{2\sigma}p_{m-1}. \tag{158}$$

Observe that the second and third terms appeared similarly in Eq. (150).

$$0 = aDb_z(D) + bb_x(D) - \lambda b_y(D) + \frac{1}{2}\mathcal{J}b_y(D)$$

$$= a\sum_{n=0}^{\infty} b_n^z \int dD\, DG_n(D)He_m^{[\sigma]}(D) + b\sum_{n=0}^{\infty} b_n^x \int dD\, G_n(D)He_m^{[\sigma]}(D) - \lambda\sum_{n=0}^{\infty} b_n^y \int dD\, G_n(D)He_m^{[\sigma]}(D)$$

$$+ \frac{\gamma}{2}\sum_{n=0}^{\infty} nb_n^y \delta_{n,m} n!\sigma^n$$

$$= a\sum_{n=0}^{\infty} b_n^z \int dD\, (G_{n+1}(D) + \sigma nG_{n-1}(D))He_m^{[\sigma]}(D) + bb_n xm!\sigma^m - \lambda b_m^y m!\sigma^m - \frac{\gamma}{2}b_m^y mm!\sigma^m$$

$$= a\sum_{n=0}^{\infty} b_n^z(\delta_{n+1,m}(n+1)!\sigma^{n+1} + \delta_{n-1,m} n!\sigma^n) + bb_n xm!\sigma^m - \lambda b_m^y m!\sigma^m - \frac{\gamma}{2}b_m^y mm!\sigma^m$$

$$= ab_{m-1}^z + a(m+1)\sigma b_{m+1}^y + bb_m^x - \lambda b_m^y - \frac{\gamma}{2}mb_m^y. \tag{159}$$

The fourth equation is almost equal to the third with one less term

$$0 = -aDb_y(D) - \lambda b_z(D) + \frac{1}{2}\mathcal{J}b_z(D)$$

$$= -a\sum_{n=0}^{\infty} b_n^y \int dD\, DG_n(D)He_m^{[\sigma]}(D) - \lambda b_m^z m!\sigma^m - \frac{\gamma}{2}b_m^z mm!\sigma^m$$

$$= -a\sum_{n=0}^{\infty} b_n^y(\delta_{n+1,m}(n+1)!\sigma^{n+1} + \delta_{n-1,m} n!\sigma^n) - \lambda b_m^z m!\sigma^m - \frac{\gamma}{2}b_m^z mm!\sigma^m$$

$$= -ab_{m-1}^y - a(m+1)\sigma b_{m+1}^y - \lambda b_m^z - \frac{\gamma}{2}mb_m^z \tag{160}$$

H Solving the system of linear equations numerically

The approach we use for numerically solving the systems of linear equations in Sec. 4 is to make a cut-off after the first n linear equations and then solve the resulting system of $3n - 1$ in the first system or $4n - 1$ linear equations in the second system ($3n - 1/4n - 1$ because the first line for $m = 0$ is just $0 = 0$).

When using the first n linear equations for every line in Eq. 67/Eq. 89, we are left with $3n - 1/4n - 1$ equations but $3n + 1/4n + 1$ unknowns because both b_{n+1}^z and b_{n+1}^x show up in the third and fourth line for $m = n$. This means we have an overdetermined system of linear equations. To solve this, we make the approximation of setting $b_{n+1}^x = b_{n+1}^x = 0$ to get back to a well-defined system of equations. This is a negligible approximation for high cut-off since both b_m^x and b_m^z have to be zero sequences as the sums $b_x(D) = \sum b_m^x G_m(D)$ and $b_z(D) = \sum b_m^z G_m(D)$ converge for all values of D.

This means we are left with a well-defined system of equations for the unknowns, which can be solved with standard numerical methods.

I   Calculating heat, work and change in measurement energy

In this chapter, we calculate heat, work, and change in measurement energy in both quantum systems in the steady state, found in Eq. 73 and Eq. 94. The non-steady state result can be found 1-2 steps before the last line in each calculation.

I.1   First quantum system

In this subsection, we use the following notation to differentiate between the rotating and lab frames.

$$\left\langle \hat{O} \right\rangle_{\text{lab}} = \int dD \, \text{Tr}\{\hat{O}\hat{\rho}_t(D)\}, \qquad \left\langle \hat{O} \right\rangle = \int dD \, \text{Tr}\{\hat{O}\hat{\chi}(D)\}, \qquad b_i(D) = \sum b_n^i G_n(D) = \text{Tr}\{\hat{\chi}(D)\hat{\sigma}_i\}. \tag{161}$$

Based on Eq. (14) and Eq. 20, we calculate power and change in measurement energy in the lab frame by transforming the quantities we calculated in the rotating frame back into the lab frame.

$$
\begin{aligned}
\gamma\langle\mathcal{A}(D)\partial_D\hat{H}(D,t)\rangle_{\text{lab}} &= \frac{\gamma}{2}\langle\hat{A}\partial_D\hat{H}(D,t) - D\partial_D\hat{H}(D,t) + \partial_D\hat{H}(D,t)\hat{A} - D\partial_D\hat{H}(D,t)\rangle_{\text{lab}} \\
&= \int dD \, \frac{\gamma}{2}\text{Tr}\{\hat{A}\partial_D\hat{H}(D,t)\hat{\rho}_t(D) - 2D\partial_D\hat{H}(D,t)\hat{\rho}_t(D) + \partial_D\hat{H}(D,t)\hat{A}\hat{\rho}_t(D)\} \\
&= \int dD \, \frac{\gamma}{2}\text{Tr}\{\hat{U}\hat{A}\hat{U}^\dagger\hat{U}\partial_D\hat{H}\hat{U}^\dagger\hat{U}\hat{\rho}\hat{U}^\dagger - 2D\hat{U}\partial_D\hat{H}\hat{U}^\dagger\hat{U}\hat{\rho}\hat{U}^\dagger + \hat{U}\partial_D\hat{H}\hat{U}^\dagger\hat{U}\hat{A}\hat{U}^\dagger\hat{U}\hat{\rho}\hat{U}^\dagger) \\
&= \frac{\gamma g}{2}\int dD \, \text{Tr}\{\hat{\sigma}_x\hat{\sigma}_y\hat{\chi} - 2D\hat{\sigma}_y\hat{\chi} + \hat{\sigma}_y\hat{\sigma}_x\hat{\chi}\} \\
&= -\gamma g\int dD \, D b_y(D) = -\gamma g\int dD \, D\sum_{n=0}^{\infty} b_n^y G_n(D) \\
&= \gamma g\int dD \, \sum_{n=0}^{\infty} b_n^y(-\sigma)G_{n-1}(D) \\
&= -\gamma g\sigma\int dD \, \sum_{n=0}^{\infty} b_n^y He_{n-1}^{[\sigma]}He_0^{[\sigma]}e^{\frac{-D^2}{2\sigma}}\frac{1}{\sqrt{2\pi\sigma}} \\
&= -\gamma g\sigma\int dD \, \sum_{n=0}^{\infty} b_n^y\delta_{n-1,0}\sigma^{n-1} \\
&= -\gamma g\sigma b_1^y = 0. \tag{162}
\end{aligned}
$$

Where we used that in the rotating frame we measure $\hat{\sigma}_x = \hat{U}\hat{A}\hat{U}^\dagger$ and that $\partial_D\hat{U}\hat{H}\hat{U}^\dagger = g\hat{\sigma}_y$. We used partial integration for $G_n(D)$ in the fifth line; see Eq. (144). In the seventh line, remember that $He_0^{[\sigma]} = 1$.

$$
\begin{aligned}
\langle P\rangle = \langle\partial_t\hat{H}(D,t)\rangle_{\text{lab}} &= \int dD \, \text{Tr}\{\hat{U}\partial_t\hat{H}\hat{U}^\dagger\hat{U}\hat{\rho}\hat{U}^\dagger\} \\
&= \int dD \, \text{Tr}\{-gD\Delta\hat{\sigma}_x\hat{\chi}\} \\
&= -g\Delta\int dD \, D b_x(D) \\
&= -g\Delta\sigma b_1^x = \lambda\Delta b_0^z. \tag{163}
\end{aligned}
$$

We used here that $\hat{U}\partial_t\hat{H}\hat{U}^\dagger = -gD\Delta\hat{\sigma}_x$ and again made partial integration to remove the D prefactor. In the last step, we use the linear equation Eq. (67).

$$
\begin{aligned}
\langle \dot{E}_M \rangle = \lambda \langle \mathcal{D}[\hat{A}]\hat{H}(D,t)\rangle_{lab} &= \lambda \langle \hat{A}\hat{H}\hat{A} - \frac{1}{2}\hat{A}\hat{A}\hat{H} - \frac{1}{2}\hat{H}\hat{A}\hat{A}\rangle_{lab} \\
&= \lambda \int dD \ \mathrm{Tr}\{\hat{U}\hat{A}\hat{U}^\dagger\hat{U}\hat{H}\hat{U}^\dagger\hat{U}\hat{A}\hat{U}^\dagger\hat{U}\hat{\rho}\hat{U}^\dagger - \frac{1}{2}\hat{U}\hat{A}\hat{U}^\dagger\hat{U}\hat{A}\hat{U}^\dagger\hat{U}\hat{H}\hat{U}^\dagger\hat{U}\hat{\rho}\hat{U}^\dagger \\
&\quad - \frac{1}{2}\hat{U}\hat{H}\hat{U}^\dagger\hat{U}\hat{A}\hat{U}^\dagger\hat{U}\hat{A}\hat{U}^\dagger\hat{U}\hat{\rho}\hat{U}^\dagger\} \\
&= \lambda \int dD \ \mathrm{Tr}\{-\frac{\Delta}{2}\hat{\sigma}_z\hat{\chi} - gD\hat{\sigma}_y\hat{\chi} - \frac{\Delta}{2}\hat{\sigma}_z\hat{\chi} - gD\hat{\sigma}_y\hat{\chi}\} \\
&= \lambda \int dD \ \mathrm{Tr}\{-\Delta\hat{\sigma}_z\hat{\chi} - 2gD\hat{\sigma}_y\hat{\chi}\} \\
&= -\lambda \left(\Delta\langle\hat{\sigma}_z\rangle + 2g\langle D\hat{\sigma}_y\rangle \right) \\
&= -\lambda\Delta b_0^z - 2\lambda g\sigma b_1^y = -\lambda\Delta b_0^z.
\end{aligned}
\tag{164}
$$

This means we have $\langle P \rangle = -\langle \dot{E}_M \rangle = \lambda\Delta b_0^z$ in the steady state.

I.2 Second quantum system

Based on Eq. (14), we calculate power and change in measurement energy in the steady state.

$$
\begin{aligned}
\langle P \rangle = \gamma\langle \mathcal{A}(D)\partial_D\hat{H}(D,t)\rangle &= \frac{\gamma}{2}\langle \hat{A}\partial_D\hat{H} - 2D\partial_D\hat{H} + \partial_D\hat{H}\hat{A}\rangle \\
&= -\frac{\gamma a}{2}\langle \hat{\sigma}_x\hat{\sigma}_x - 2D\hat{\sigma}_x + \hat{\sigma}_x\hat{\sigma}_x\rangle \\
&= -\gamma a\left(\int dD\, P(D) - \int dD\, Db_x(D) \right) \\
&= -\gamma a(1 - \sigma b_1^x) = 2\lambda b b_0^z.
\end{aligned}
\tag{165}
$$

Where we used that $\partial_D\hat{H}(D) = -a\hat{\sigma}_x$. In the last step, we used the linear equation Eq. (89).

$$
\begin{aligned}
\langle \dot{E}_M \rangle = \lambda\langle \mathcal{D}[\hat{A}]\hat{H}(D,t)\rangle &= \lambda\langle \hat{A}\hat{H}\hat{A} - \frac{1}{2}\hat{A}\hat{A}\hat{H} - \frac{1}{2}\hat{H}\hat{A}\hat{A}\rangle \\
&= \lambda\langle \hat{\sigma}_x(-aD\hat{\sigma}_x + b\hat{\sigma}_z)\hat{\sigma}_x + aD\hat{\sigma}_x - b\hat{\sigma}_z\rangle \\
&= -2\lambda b\langle\hat{\sigma}_z\rangle = -2\lambda b b_0^z.
\end{aligned}
\tag{166}
$$

J Special cases for the two Quantum systems under Feedback control

In the first system for $g = 0$ or the second system for $b = 0$, we find the same general expression for b_m^i and p_m; see Eq. (77) or Eq. (98). We can now find explicit expressions for the functions $b_x(D)$ and $P(D)$ when using the following generating function of the Hermite polynomials

$$
\sum_{n=0}^{\infty} \frac{t^n}{n!}He_n(x) = e^{xt-t^2/2} \implies \sum_{n=0}^{\infty} \frac{t^n}{n!}He_n^{[\sigma]}(x) = \sigma^{n/2}e^{xt/\sqrt{\sigma}-t^2/2}
\tag{167}
$$

We use this expression for $t = \frac{1}{\sqrt{\sigma}}$ to find

$$
\sum_{n=0}^{\infty} \frac{1}{\sigma^n n!}He_n^{[\sigma]}(x) = e^{x/\sigma - 1/2\sigma}
\tag{168}
$$

Now we can calculate a closed form for $P(D)$ and $b_x(D)$ using Eq. (168) and Eq. (70)

$$
\begin{aligned}
P(D) &= \frac{1}{\sqrt{2\pi\sigma}} e^{\frac{-D^2}{2\sigma}} \sum_{m=0}^{\infty} He_m^{[\sigma]}(D) p_m \\
&= \frac{1}{\sqrt{2\pi\sigma}} e^{\frac{-D^2}{2\sigma}} \sum_{m \text{ even}}^{\infty} \frac{1}{m!\sigma^m} He_m^{[\sigma]}(D) \\
&= \frac{1}{\sqrt{2\pi\sigma}} e^{\frac{-D^2}{2\sigma}} \sum_{m=0}^{\infty} \frac{1}{m!\sigma^m} \left(\frac{1}{2} He_m^{[\sigma]}(D) + (-1)^m \frac{1}{2} He_m^{[\sigma]}(D) \right) \\
&= \frac{1}{\sqrt{2\pi\sigma}} e^{\frac{-D^2}{2\sigma}} \sum_{m=0}^{\infty} \frac{1}{m!\sigma^m} \left(\frac{1}{2} He_m^{[\sigma]}(D) + \frac{1}{2} He_m^{[\sigma]}(-D) \right) \\
&= \frac{1}{\sqrt{2\pi\sigma}} \left(\frac{1}{2} e^{(2D-D^2-1)/2\sigma} + \frac{1}{2} e^{(-2D-D^2-1)/2\sigma} \right) \\
&= \frac{1}{2\sqrt{2\pi\sigma}} \left(e^{-(D-1)^2/2\sigma} + e^{-(D+1)^2/2\sigma} \right).
\end{aligned}
\tag{169}
$$

$$
\begin{aligned}
b_x(D) &= \frac{1}{\sqrt{2\pi\sigma}} e^{\frac{-D^2}{2\sigma}} \sum_{m=0}^{\infty} He_m^{[\sigma]}(D) p_m \\
&= \frac{1}{\sqrt{2\pi\sigma}} e^{\frac{-D^2}{2\sigma}} \sum_{m \text{ odd}}^{\infty} \frac{1}{m!\sigma^m} He_m^{[\sigma]}(D) \\
&= \frac{1}{\sqrt{2\pi\sigma}} e^{\frac{-D^2}{2\sigma}} \sum_{m=0}^{\infty} \frac{1}{m!\sigma^m} \left(\frac{1}{2} He_m^{[\sigma]}(D) - (-1)^m \frac{1}{2} He_m^{[\sigma]}(D) \right) \\
&= \frac{1}{\sqrt{2\pi\sigma}} e^{\frac{-D^2}{2\sigma}} \sum_{m=0}^{\infty} \frac{1}{m!\sigma^m} \left(\frac{1}{2} He_m^{[\sigma]}(D) - \frac{1}{2} He_m^{[\sigma]}(-D) \right) \\
&= \frac{1}{\sqrt{2\pi\sigma}} \left(\frac{1}{2} e^{(2D-D^2-1)/2\sigma} - \frac{1}{2} e^{(-2D-D^2-1)/2\sigma} \right) \\
&= \frac{1}{2\sqrt{2\pi\sigma}} \left(e^{-(D-1)^2/2\sigma} - e^{-(D+1)^2/2\sigma} \right).
\end{aligned}
\tag{170}
$$

K   Differential equation for the fast detector limit

In this section, we derive the differential equation for the fast detector limits Eq. (84) and Eq. (102).
For the first system, we start with Eq. (81) and then calculate the terms one by one using (82). Then multiplying with $\hat{\sigma}_i$ and taking the trace leaves us with the three promised differential equations (84).

$$
\begin{aligned}
-ig[\hat{\sigma}_y, \mathcal{A}\hat{\rho}_t] &= -ig[\hat{\sigma}_y, \frac{1}{2}(\hat{\sigma}_x\hat{\rho}_t + \hat{\rho}_t\hat{\sigma}_x)] \\
&= -\frac{1}{2} ig \left(\hat{\sigma}_y\hat{\sigma}_x\hat{\rho}_t + \hat{\sigma}_y\hat{\rho}_t\hat{\sigma}_x - \hat{\rho}_t\hat{\sigma}_x\hat{\sigma}_y - \hat{\sigma}_x\hat{\rho}_t\hat{\sigma}_y \right) \\
&= -\frac{ig}{2} \left(\hat{\sigma}_y\hat{\sigma}_x \left(\frac{1}{2} (\mathbb{1} + B_x\hat{\sigma}_x + B_y\hat{\sigma}_y + B_z\hat{\sigma}_z) \right) - \left(\frac{1}{2} (\mathbb{1} + B_x\hat{\sigma}_x + B_y\hat{\sigma}_y + B_z\hat{\sigma}_z) \right) \hat{\sigma}_x\hat{\sigma}_y \right) \\
&= -g\hat{\sigma}_z.
\end{aligned}
\tag{171}
$$

$$
\begin{aligned}
\lambda\mathcal{D}[\hat{\sigma}_x]\hat{\rho}_t &= \lambda(\hat{\sigma}_x\hat{\rho}_t\hat{\sigma}_x - \hat{\rho}_t) \\
&= \lambda(\hat{\sigma}_x \left(\frac{1}{2} (\mathbb{1} + B_x\hat{\sigma}_x + B_y\hat{\sigma}_y + B_z\hat{\sigma}_z) \right) \hat{\sigma}_x - \frac{1}{2} (\mathbb{1} + B_x\hat{\sigma}_x + B_y\hat{\sigma}_y + B_z\hat{\sigma}_z)) \\
&= -\lambda(B_y\hat{\sigma}_y + B_z\hat{\sigma}_z).
\end{aligned}
\tag{172}
$$

46

$$\frac{1}{4\lambda}\mathcal{D}[g\hat{\sigma}_y]\hat{\rho}_t = \frac{g^2}{4\lambda}(\hat{\sigma}_y\hat{\rho}_t\hat{\sigma}_y - \hat{\rho}_t)$$

$$= \frac{g^2}{4\lambda}(\hat{\sigma}_y\left(\frac{1}{2}\left(\mathbb{1} + B_x\hat{\sigma}_x + B_y\hat{\sigma}_y + B_z\hat{\sigma}_z\right)\right)\hat{\sigma}_y - \left(\frac{1}{2}\left(\mathbb{1} + B_x\hat{\sigma}_x + B_y\hat{\sigma}_y + B_z\hat{\sigma}_z\right)\right))$$

$$= -\frac{g^2}{4\lambda}(B_x\hat{\sigma}_x + B_z\hat{\sigma}_z). \tag{173}$$

For the second system, we make the same calculations to find the three differential equations (102).

$$-ib[\hat{\sigma}_z, \hat{\rho}_t] = -ib(\hat{\sigma}_z\left(\frac{1}{2}\left(\mathbb{1} + B_x\hat{\sigma}_x + B_y\hat{\sigma}_y + B_z\hat{\sigma}_z\right)\right) - \left(\frac{1}{2}\left(\mathbb{1} + B_x\hat{\sigma}_x + B_y\hat{\sigma}_y + B_z\hat{\sigma}_z\right)\right)\hat{\sigma}_z$$

$$= b(B_x\hat{\sigma}_y - B_y\hat{\sigma}_y). \tag{174}$$

$$ia[\hat{\sigma}_x, \mathcal{A}\hat{\rho}_t] = -ia[\hat{\sigma}_x, \frac{1}{2}(\hat{\sigma}_x\hat{\rho}_t + \hat{\rho}_t\hat{\sigma}_x)]$$

$$= \frac{1}{2}ia\left(\hat{\sigma}_x\hat{\sigma}_x\hat{\rho}_t + \hat{\sigma}_x\hat{\rho}_t\hat{\sigma}_x - \hat{\rho}_t\hat{\sigma}_x\hat{\sigma}_x - \hat{\sigma}_x\hat{\rho}_t\hat{\sigma}_x\right)$$

$$= \frac{ig}{2}\left(\hat{\sigma}_x\hat{\sigma}_x\left(\frac{1}{2}\left(\mathbb{1} + B_x\hat{\sigma}_x + B_y\hat{\sigma}_y + B_z\hat{\sigma}_z\right)\right) - \left(\frac{1}{2}\left(\mathbb{1} + B_x\hat{\sigma}_x + B_y\hat{\sigma}_y + B_z\hat{\sigma}_z\right)\right)\hat{\sigma}_x\hat{\sigma}_y\right)$$

$$= 0. \tag{175}$$

$$\lambda\mathcal{D}[\hat{\sigma}_x]\hat{\rho}_t = \lambda(\hat{\sigma}_x\hat{\rho}_t\hat{\sigma}_x - \hat{\rho}_t)$$

$$= \lambda(\hat{\sigma}_x\left(\frac{1}{2}\left(\mathbb{1} + B_x\hat{\sigma}_x + B_y\hat{\sigma}_y + B_z\hat{\sigma}_z\right)\right)\hat{\sigma}_x - \frac{1}{2}\left(\mathbb{1} + B_x\hat{\sigma}_x + B_y\hat{\sigma}_y + B_z\hat{\sigma}_z\right))$$

$$= -\lambda(B_y\hat{\sigma}_y + B_z\hat{\sigma}_z). \tag{176}$$

$$\frac{1}{4\lambda}\mathcal{D}[a\hat{\sigma}_x]\hat{\rho}_t = \frac{a^2}{4\lambda}(\hat{\sigma}_x\hat{\rho}_t\hat{\sigma}_x - \hat{\rho}_t)$$

$$= \frac{a^2}{4\lambda}(\hat{\sigma}_x\left(\frac{1}{2}\left(\mathbb{1} + B_x\hat{\sigma}_x + B_y\hat{\sigma}_y + B_z\hat{\sigma}_z\right)\right)\hat{\sigma}_x - \left(\frac{1}{2}\left(\mathbb{1} + B_x\hat{\sigma}_x + B_y\hat{\sigma}_y + B_z\hat{\sigma}_z\right)\right))$$

$$= -\frac{a^2}{4\lambda}(B_y\hat{\sigma}_y + B_z\hat{\sigma}_z). \tag{177}$$

After finding the three differential equations (102), we can write them in the form

$$\partial_t \begin{pmatrix} B_x(t) \\ B_y(t) \\ B_z(t) \end{pmatrix} = \begin{pmatrix} 0 & -2b & 0 \\ 2b & -\lambda - \frac{a^2}{2\lambda} & 0 \\ 0 & 0 & -\lambda - \frac{a^2}{2\lambda} \end{pmatrix} \begin{pmatrix} B_x(t) \\ B_y(t) \\ B_z(t) \end{pmatrix}. \tag{178}$$

By finding the three eigenvalues λ_i and corresponding eigenvectors $\vec{e_i}$ we can write down the solution

$$\begin{pmatrix} B_x(t) \\ B_y(t) \\ B_z(t) \end{pmatrix} = c_1 e^{\lambda_1 t}\vec{e_1} + c_2 e^{\lambda_2 t}\vec{e_2} + c_3 e^{\lambda_3 t}\vec{e_3}. \tag{179}$$

To keep things simple, we calculate here only the case where $a = 1, b = 1, \lambda = 1$. Then

$$\begin{pmatrix} B_x(t) \\ B_y(t) \\ B_z(t) \end{pmatrix} = c_1 e^{-5/2t}\begin{pmatrix} 0 \\ 0 \\ 1 \end{pmatrix} + c_2 e^{1/4(-5+i\sqrt{39})t}\begin{pmatrix} 1/8(5 + i\sqrt{39}) \\ 1 \\ 0 \end{pmatrix} + c_3 e^{1/4(-5-i\sqrt{39})t}\begin{pmatrix} 1/8(5 - i\sqrt{39}) \\ 1 \\ 0 \end{pmatrix}. \tag{180}$$

This means when starting in the mixed state $B_x(0) = B_y(0) = B_z(0) = -1/\sqrt{3}$ we find

$$\begin{pmatrix} B_x(t) \\ B_y(t) \\ B_z(t) \end{pmatrix} = \begin{pmatrix} \frac{1}{39}e^{-5/4t}\left(3\sqrt{13}\sin\left(\frac{\sqrt{39}t}{4}\right) - 13\sqrt{3}\cos\left(\frac{\sqrt{39}t}{4}\right)\right) \\ -\frac{1}{39}e^{-5/4t}\left(3\sqrt{13}\sin\left(\frac{\sqrt{39}t}{4}\right) + 13\sqrt{3}\cos\left(\frac{\sqrt{39}t}{4}\right)\right) \\ -\frac{1}{\sqrt{3}}e^{-5/4t} \end{pmatrix}. \tag{181}$$

L   Numerical plots of the fast detector limit

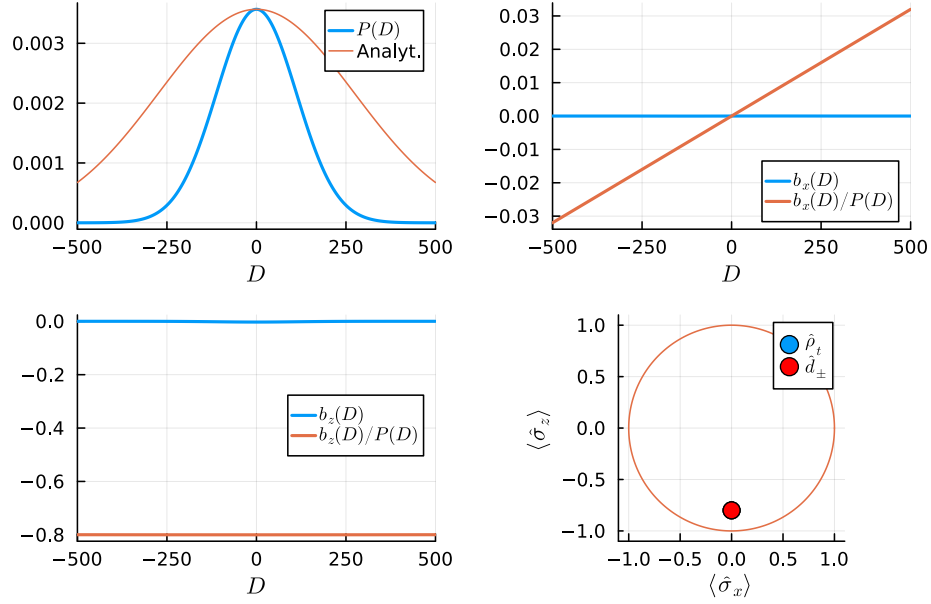In this section, we have two examples of the numerical solutions we find in the limit $\gamma \to \infty$.

Figure 19: Numerical solution for the steady state of the first system in the limit $\gamma \to \infty$. The parameter choice here is $g = 1, \lambda = 1, \gamma = 100000$. As we can see, the $\langle \hat{\sigma}_z \rangle$ value is almost exactly $-4/5$, which is the steady state for the analytic solution we have found.
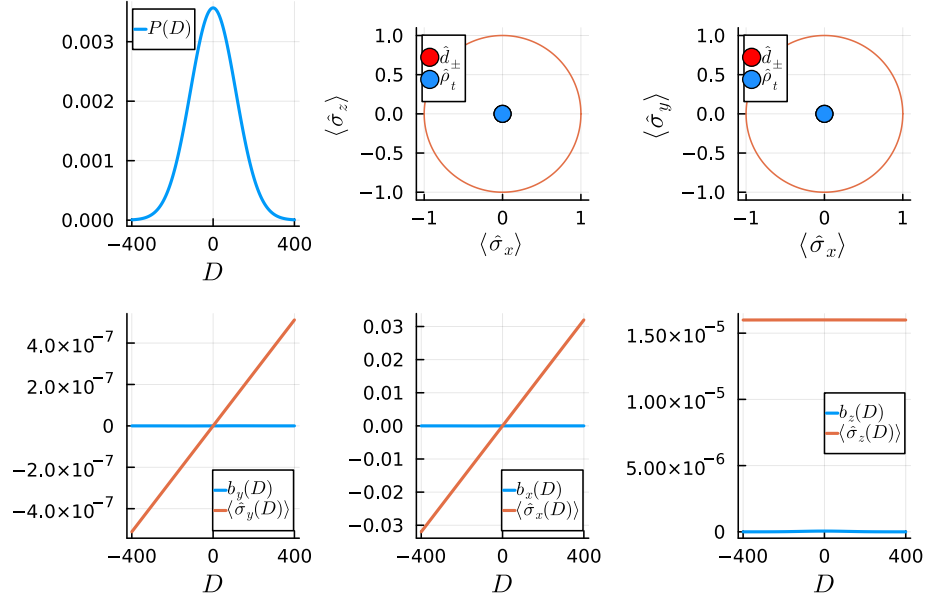

Figure 20: Numerical solution for the steady state of the second system in the limit $\gamma \to \infty$. The parameter choice here is $a = b = 1, \lambda = 1, \gamma = 100000$. As we can see, the $\langle \hat{\sigma}_z \rangle$ value is almost exactly zero, which is the steady state for the analytic solution we have found.

M   Feedback independent Hamiltonain

In this section, we calculate the precession introduced by a static Hamiltonian for the second system.

The first step to finding a differential equation for $\hat{\rho}_t$ for $\hat{H} = -a\hat{\sigma}_x + b\hat{\sigma}_y$ is to first use Eq. 88 for a fixed $D = D_\pm$ and $\lambda = 0$ and then integrate out the measurement result by $\int dD$. We will also use the following two expressions

$$\int dD\,\mathrm{Tr}\{\hat{\rho}_t(D)\hat{\sigma}_i\} = \mathrm{Tr}\{\hat{\rho}_t\hat{\sigma}_i\} = \langle\hat{\sigma}_i\rangle(t),$$

$$\int dD\,\partial_D^j\,\mathrm{Tr}\{\hat{\rho}_t(D)\hat{\sigma}_i\} = \partial_D^{j-1}\,\mathrm{Tr}\{\hat{\rho}_t(D)\hat{\sigma}_i\}\,\big|_{D=-\infty}^{D=\infty} = 0\,, \quad \text{for } j = \{1,2\}. \tag{182}$$

After the integration, we are left with three coupled differential equations

$$\begin{aligned}
\partial_t\langle\hat{\sigma}_x\rangle(t) &= -b\langle\hat{\sigma}_y\rangle(t),\\
\partial_t\langle\hat{\sigma}_y\rangle(t) &= a\langle\hat{\sigma}_z\rangle(t) + b\langle\hat{\sigma}_x\rangle(t),\\
\partial_t\langle\hat{\sigma}_z\rangle(t) &= -a\langle\hat{\sigma}_y\rangle(t).
\end{aligned} \tag{183}$$

We can rewrite these three equations into

$$\partial_t \begin{pmatrix} \langle\hat{\sigma}_x\rangle \\ \langle\hat{\sigma}_y\rangle \\ \langle\hat{\sigma}_z\rangle \end{pmatrix} = \begin{pmatrix} 0 & -b & 0 \\ b & 0 & a \\ 0 & -a & 0 \end{pmatrix} \begin{pmatrix} \langle\hat{\sigma}_x\rangle \\ \langle\hat{\sigma}_y\rangle \\ \langle\hat{\sigma}_z\rangle \end{pmatrix}. \tag{184}$$

By finding the three eigenvalues λ_i and corresponding eigenvectors $\vec{e}_i$ we can write down the solution

$$\begin{pmatrix} \langle\hat{\sigma}_x\rangle(t) \\ \langle\hat{\sigma}_y\rangle(t) \\ \langle\hat{\sigma}_z\rangle(t) \end{pmatrix} = Ae^{\lambda_1 t}\vec{e_1} + Be^{\lambda_2 t}\vec{e_2} + Ce^{\lambda_3 t}\vec{e_3}. \tag{185}$$

An initial starting condition then determines the constants A, B, C.